Characterisation of cold-selective lamina I spinal projection neurons

Aimi N. Razlan[1,4], Wenhui Ma[1,4], Allen C. Dickie[1,4], Erika Polgár[1,4], Anna McFarlane[1], Mansi Yadav[1], Andrew H. Cooper[1], Douglas Strathdee[2], Masahiko Watanabe[3], Andrew M. Bell[1], Andrew J. Todd[1]*, Junichi Hachisuka[1]*

[1]School of Psychology and Neuroscience, College of Medical, Veterinary and Life Sciences, University of Glasgow, Glasgow G12 8QQ, UK

[2]School of Cancer Sciences, College of Medical, Veterinary and Life Sciences, University of Glasgow, Bearsden G61 1BD UK

[3]Department of Anatomy, Hokkaido University School of Medicine, Sapporo 060-8638, Japan

[4]Equal contribution

*Corresponding Authors: Andrew.Todd@glasgow.ac.uk and Junichi.Hachisuka@Glasgow.ac.uk

Click here to enter text.

ABSTRACT

Skin cooling is detected by primary afferents that express the Trpm8 channel, but how this information is conveyed to the brain remains poorly understood. We have previously identified a population of lamina I projection neurons belonging to the anterolateral system (ALS) that receive numerous contacts from Trpm8-expressing primary afferents. Here, using a semi-intact somatosensory preparation, we provide evidence that these cells correspond to the cold-selective ALS neurons identified in previous physiological studies. We also confirm the presence of synapses from Trpm8 afferents onto these cells at the ultrastructural level and with optogenetics. Based on our previous transcriptomic findings, we identify calbindin as a molecular marker, and show that this can be used to target the cold-selective ALS neurons for anterograde tracing studies. We provide evidence that they project to brain regions that have been implicated in thermosensation: the rostralmost part of the lateral parabrachial area, the caudal part of the periaqueductal grey matter, and the posterior triangular and ventral posterolateral nuclei of the thalamus. Our findings provide important insights into the organisation of neuronal circuits that underlie thermoregulation and the perception of cold stimuli applied to the skin.

Click here to enter text.

INTRODUCTION

The anterolateral system (ALS) consists of spinal cord neurons that project to various brain regions, including the caudal ventrolateral medulla (CVLM), the nucleus of the solitary tract (NTS), the lateral parabrachial area (LPB), the periaqueductal grey matter (PAG), the superior colliculus and the thalamus. ALS neurons are required for the perception of pain, itch and skin temperature, as shown by the loss of these sensations on the side contralateral to an anterolateral cordotomy[1,2]. Although axons belonging to this pathway ascend in the anterolateral quadrant in humans, they are located in the dorsolateral white matter in rodents[3-6]. ALS neurons account for only a small proportion (probably less than 1%) of spinal cord neurons[7,8] and are unevenly distributed, with a relatively high density in lamina I and the lateral spinal nucleus (LSN), and scattered cells in deeper laminae (III-VII) and around the central canal[9-12]. ALS neurons are functionally heterogeneous, and we recently identified 5 distinct transcriptomic populations, which we named ALS1-5[13]. This was based on single-nucleus RNA sequencing of a major subset of these cells, those that transiently express the transcription factor Phox2a during development[14].

Perception of skin cooling is dependent on primary afferent neurons that express the Trpm8 channel[15-19], and these terminate mainly in lamina I of the spinal cord[20-22]. Consistent with this, it has been shown that many lamina I projection neurons respond to cool or cold stimuli applied to the skin, with a distinctive subset of “cold-selective” neurons responding predominantly or exclusively to skin cooling[23-33].

How information is transmitted from Trpm8-expressing primary afferent neurons to these cold-selective lamina I ALS cells is currently not known, although a recent report has suggested that this occurs via a dedicated population of excitatory interneurons[34]. However, we had previously identified a population of lamina I ALS neurons that received dense synaptic input from Trpm8-expressing primary afferents[13]. These neurons had dendrites that were intimately associated with bundles of Trpm8-positive afferents, while their cell bodies generally also received numerous contacts, and were sometimes surrounded by these afferents. We therefore proposed that these cells correspond to the cold-selective neurons described above, and also provided evidence that they belonged to the ALS3 population[13].

The aims of this study were to characterise and validate the Trpm8^{Flp} mouse line that we had used to reveal this input, to confirm the presence of synaptic input, and to test the prediction that the lamina I projection neurons with dense synaptic input from Trpm8-

Click here to enter text.

expressing primary afferents do indeed correspond to the cold-selective population described in physiological studies[23-33]. In addition, since Calb1 (which encodes the calcium-binding protein calbindin) is one of the top differentially expressed genes in the ALS3 population, we used mice in which Cre recombinase is targeted to the Calb1 locus (Calb1^{Cre}) to investigate the projections of the ALS3 cells to the brain.

RESULTS

Validation of Trpm8^{Flp} mouse line and characterisation of Flp-expressing cells.

Trpm8^{Flp} mice were crossed with the Flp reporter line RCE:FRT to generate Trpm8^{Flp};RCE:FRT mice, in which cells that express Flp at any stage during development are labelled with GFP. Tissue was obtained from mice aged between 5-9 weeks for this part of the study. We used a stereological technique to quantify neurons in an L4 dorsal root ganglion (DRG) from 3 of these mice and found that 5.7% (range 5.4-6.7%) of all DRG neurons contained GFP (Figure 1A). We then performed fluorescence *in situ* hybridisation (FISH) to examine the extent of overlap between GFP and *Trpm8* mRNA (Figure 1B). In DRGs from 3 mice, we found that 92% (88%-98%) of GFP-containing cells had *Trpm8* message, while 83% (80%-86%) of cells with *Trpm8* were GFP-positive. These findings show a high degree of fidelity in the Trpm8^{Flp} line, and are consistent with the reported expression of *Trpm8* mRNA in 5-10% of mouse DRG cells[15]. We also used this tissue to determine the soma size of the GFP-positive cells (Figure 1C), and found that these were small, with a mean diameter of 14.6 µm (± 3.4 µm, SD), showing a very similar size range to that reported for cells captured with a different Trpm8^{Flp} mouse line[35]. Trpm8-positive cells that lacked GFP, as well as the few GFP-labelled cells that lacked *Trpm8* mRNA, showed a similar size distribution.

Transcriptomic studies have demonstrated that Trpm8-expressing primary afferents can co-express certain genes that serve as markers for primary afferent populations, such as Slc17a8 (which encodes Vglut3), Trpv1 and Tac1 (the gene coding for substance P), but lack other neuropeptides such as calcitonin gene-related peptide (CGRP) and somatostatin[36,37]. We therefore performed immunohistochemistry to look for expression of the corresponding proteins/peptides in dorsal root ganglia from 3 mice in each case. We found that 11.9% (9.8-13.8%) of GFP-containing cells were immunoreactive for Vglut3 and 26.4% (22.4-30.9%) for Trpv1 (Figure 1–figure supplement 1A-D). Among the neuropeptides, we found minimal co-localisation with CGRP (mean 2.5%, range 1.4-4.5%) and none with somatostatin. However, 56% (range 55.8-56.3%) of the GFP cells contained

Click here to enter text.

substance P, although this was expressed at relatively low levels (Figure 1–figure supplement 1G-M). These results are therefore consistent with the transcriptomic findings described above[36,37].

Central projections of Trpm8-expressing primary afferents have been shown to terminate mainly in lamina I[20-22], and we found a similar pattern in the spinal cords of Trpm8^{Flp};RCE:FRT mice, with the great majority of GFP-labelled axons remaining in lamina I, and very few passing ventrally (Figure 2). A similar pattern of labelling was observed in all spinal segments examined. We had previously noted that when lamina I was viewed in horizontal sections, Trpm8 afferents were arranged in interweaving bundles that frequently followed the dendrites of a distinctive subset of projection neurons[13]. Consistent with this, we found that Trpm8 afferents labelled with GFP showed a discontinuous arrangement within lamina I when viewed in transverse sections and did not occupy the whole medio-lateral extent of the lamina (Figure 2). The GFP-labelled afferents did not show any obvious restriction in the medio-lateral axis, and could be seen in medial, central and lateral parts of lamina I. Since the great majority of Trpm8-expressing afferents contain GFP in this genetic cross, it is unlikely that the large spaces between bundles of GFP-labelled afferents in lamina I are filled by Trpm8-expressing afferents that lack GFP. This “incomplete” innervation of lamina I by Trpm8 afferents is therefore likely to be genuine.

It has been reported that some lamina I projection neurons were associated with boutons that were immunoreactive for Vglut3[38] and since 12% of Trpm8 afferent cell bodies contained Vglut3, we looked for expression of the transporter in their central terminals. In transverse sections, Vglut3-immunoreactive axons formed a dense band in inner lamina II that corresponds to central terminals of C-low threshold mechanoreceptors (C-LTMRs)[39,40]. However, there were a few Vglut3-immunoreactive boutons in lamina I that were also GFP-positive, indicating that central terminals of some Trpm8-expressing primary afferents had detectable levels of the transporter (Figure 2–figure supplement 1A-F). We generated a mouse genetic cross (Phox2a::Cre;Ai9;Trpm8^{Flp};RCE:FRT) in which a subset of ALS cells express tdTomato and Trpm8 afferents express GFP. In horizontal sections from these mice we identified lamina I projection neurons that were associated with numerous GFP-labelled (Trpm8-expressing) boutons and found that some of these boutons contained Vglut3 (Figure 2–figure supplement 1G-J). The proportion of GFP-labelled boutons that contained Vglut3 varied considerably between cells. Since C-LTMRs do not appear to arborise in lamina I[35], it is likely that the Vglut3-containing boutons that

Click here to enter text.

136 have been found to contact projection neurons in this lamina[38] belong to Trpm8 afferents.
137 Even though many Trpm8-positive cell bodies showed Trpv1 and substance P
138 immunoreactivities, we were not able to detect either of these in their central terminals
139 (Figure 2–figure supplement 1K-M).
140 Although we did not investigate the distribution of GFP in the brains of
141 Trpm8^{Flp};RCE:FRT mice in detail, we noted that there was dense axonal labelling in the
142 spinal trigeminal nucleus, while scattered GFP-labelled cell bodies were present in various
143 brain regions that are known to contain Trpm8-expressing neurons, including the preoptic
144 area and the reticular nucleus of the thalamus[41] (data not shown).
145
146 **Synaptic input from Trpm8-expressing afferents to lamina I projection neurons.**
147 We had previously shown that ~20% of lamina I projection neurons retrogradely
148 labelled from the LPB received numerous contacts from GFP-labelled afferents in
149 Trpm8^{Flp};RCE:FRT mice, and that these contacts were associated with punctate staining
150 for Homer1[13] (a marker for glutamatergic synapses[42]). To reveal synapses formed
151 between Trpm8 afferents and these projection neurons at the ultrastructural level, we used
152 a combined confocal/electron microscopic method[43] on spinal cord tissue from
153 Phox2a::Cre;Ai9;Trpm8^{Flp};RCE:FRT mice. This genetic cross was chosen because we had
154 previously shown that the Phox2a-lineage includes many lamina I ALS neurons with dense
155 input from Trpm8 afferents[13]. Horizontal sections from lumbar spinal cord segments of 2 of
156 these mice were immunostained to reveal tdTomato and GFP, and 3 tdTomato-labelled
157 cells with numerous contacts from GFP-labelled axons were scanned with a confocal
158 microscope (Figure 3, Figure 3–figure supplements 1 and 2). The tissue was subsequently
159 processed with an immunoperoxidase method to label the GFP-positive axons with
160 diaminobenzidine (DAB), and examined with an electron microscope (Figure 3, Figure 3–
161 figure supplement 2). Although the cell bodies and dendrites of the projection neurons did
162 not contain an electron-dense label, they could be readily identified by their location within
163 the ultrathin sections, by their association with numerous DAB-labelled axonal boutons
164 and by the morphology of their somata and proximal dendrites (Figure 3A,B). Because of
165 the very high density of GFP-labelled boutons that were seen to contact the cells in the
166 confocal images, it was not always possible to relate individual boutons from confocal
167 images to those seen with the electron microscope. However, we were able to identify
168 numerous axosomatic and axodendritic synapses (a minimum of 10 synapses per cell)
169 between the GFP-immunoreactive boutons and the lamina I projection neurons. These

Click here to enter text.

170 could be recognised by the presence of darkening of the membranes and in some cases a
171 faint postsynaptic density, together with clustering of synaptic vesicles on the presynaptic
172 side (Figure 3B-D, Figure 3–figure supplement 2C-J). Interestingly, the synapses between
173 the GFP-containing boutons and the projection neurons generally had relatively faint
174 postsynaptic densities and only small regions where the vesicles were clustered on the
175 presynaptic side. These findings, together with our previous observation of Homer1-
176 immunoreactive puncta located between GFP-expressing afferent boutons and the cell
177 bodies and dendrites of retrogradely labelled lamina I projection neurons in
178 Trpm8^{Flp};RCE:FRT mice[13], indicate that ALS cells belonging to this population receive
179 numerous synapses from Trpm8-expressing primary afferents.
180 To provide electrophysiological evidence for synapses between Trpm8 afferents and
181 this population of lamina I ALS cells, we carried out optogenetic experiments. Two
182 Trpm8^{Flp};RCE:FRT mice received intraperitoneal injections of
183 AAV.PHP.S.Flp^{ON}.ChR2_YFP as neonates to label Trpm8-expressing primary afferents
184 with channelrhodopsin. They were then injected with AAV11.tdTomato into the CVLM or
185 LPB ~5 weeks later (Figure 3E). Whole-cell patch-clamp recordings were subsequently
186 obtained from tdTomato-labelled lamina I neurons in a whole-cord preparation. We used
187 the Trpm8^{Flp};RCE:FRT cross for these experiments in order to allow un-biased
188 identification of ALS neurons that were surrounded by Trpm8 afferents. Importantly,
189 although the viral delivery approach that we used will have specifically targeted Trpm8
190 afferents, it will not have resulted in adequate expression of channelrhodopsin in all of
191 these cells.
192 We identified 8 tdTomato cells that were densely surrounded by GFP-labelled (Trpm8)
193 afferents and found that 1 ms blue light pulses induced EPSCs in 5 of these cells (Figure
194 3E,F). We measured the latency of the first EPSC after blue light pulses (0.2 Hz) and
195 found that the latency jitter was less than 1 ms, indicating that these neurons receive
196 monosynaptic inputs[44] (Figure 3F; n = 5, Average latency: 5.8 ± 0.86 ms, latency jitter:
197 0.68 ± 0.14 ms). Note that the relatively long latency is likely to reflect the time taken for
198 action potential initiation in the Trpm8 boutons[31]. Two of the 5 neurons showed multiple
199 peaks with a larger latency jitter, indicating that there may also have been polysynaptic
200 inputs (Figure 3–figure supplement 3). It is likely that the remaining 3 cells received input
201 from Trpm8 afferents that did not express sufficiently high levels of channelrhodopsin.
202 Together, these findings demonstrate that Trpm8 afferents directly synapse onto lamina I
203 ALS cells that are surrounded by these afferents.

Click here to enter text.

204

205 **Lamina I ALS neurons that are surrounded by Trpm8 afferents are cold-selective**

206 We next tested whether the lamina I projection neurons that are densely innervated by
207 Trpm8 afferents correspond to the cold-selective neurons identified in physiological
208 studies[23-33]. To do this, we carried out whole-cell patch-clamp recordings in preparations in
209 which ALS neurons were retrogradely labelled with either mCherry or tdTomato, and
210 Trpm8 axons expressed GFP. Retrograde labelling was achieved by injecting
211 AAV9.mCherry into the CVLM or LPB of Trpm8^{Flp};RCE:FRT mice, resulting in mCherry
212 labelling, or else by injecting AAV9.Cre_GFP into the CVLM of Trpm8^{Flp};RCE:FRT;Ai9
213 mice leading to tdTomato labelling (Figure 4A). We used the semi-intact *ex vivo*
214 somatosensory preparation, in which the spinal cord, L2 and L3 roots and ganglia,
215 saphenous and femoral cutaneous nerves, and hindlimb skin are dissected in continuity
216 (Fig 4B)[31,32].

217 Visualisation of the spinal cord with filter sets for GFP or mCherry/tdTomato revealed
218 lamina I projection neurons (labelled with mCherry or tdTomato) as well as a plexus of
219 GFP-labelled (Trpm8-expressing) primary afferents (Figure 4). We recorded from 6
220 mCherry/tdTomato-labeled projection neurons that had dendrites (and in some cases also
221 cell bodies) that were clearly associated with numerous GFP-labelled afferents, as well as
222 from 5 projection neurons for which there was no clear association with these afferents.
223 We assessed the responses of these cells to a 4 g von Frey filament, hot saline (50°C),
224 and cold saline (15°C) applied to the skin[31]. All 6 of the projection neurons that had
225 numerous contacts from GFP-labelled axons responded exclusively to application of cold
226 saline. In 4 cases recordings were made in current clamp and the cells fired action
227 potentials (n = 3) or generated EPSPs (subthreshold, n = 1) following application of cold
228 saline, but showed no response to mechanical or heat stimuli (Figure 4C-E). The time
229 course of the response was consistent with that seen for cold-selective projection neurons
230 that we previously reported (Figure 4–figure supplement 1)[32]. The other two cells with
231 numerous GFP contacts were recorded in voltage clamp, and these showed EPSCs in
232 response to cold, but not mechanical or heat, stimuli. All six of these neurons were
233 therefore classified as cold-selective. The five projection neurons that were not
234 preferentially associated with GFP-labelled afferents were all recorded in current clamp
235 mode, and all of these cells exhibited action potential firing in response to mechanical
236 stimulation. Three of them also responded to heat, and one additionally to cold stimuli. The

237 five neurons that were not associated with numerous GFP-labelled afferents were
238 therefore classified as either mechano-selective or polymodal (Figure 4F-H).
239 We previously reported that cold-selective projection neurons are distinct from other
240 lamina I projection neurons[32], and a defining feature of these cells was their low frequency
241 of spontaneous EPSCs (sEPSCs). We therefore quantified sEPSC frequency and
242 amplitude in lamina I projection neurons with or without dense Trpm8 input. As expected,
243 neurons with dense Trpm8 input had significantly lower sEPSC frequencies compared to
244 those that lacked dense Trpm8 input (Figure 4–figure supplement 1). Interestingly, the
245 amplitude of sEPSCs in the projection neurons with dense Trpm8 input was smaller than
246 in those that lacked this input, which had not been observed in our previous study[32].
247 Together, these results strongly suggest that lamina I projection neurons receiving dense
248 Trpm8 afferent innervation constitute a distinct neuronal population specialised for cold
249 sensation, and correspond to the cold-selective ALS neurons identified in previous
250 studies[23-33].
251 Our anatomical studies indicate that the cells densely coated with Trpm8-expressing
252 primary afferents receive many synapses from these afferents (Figure 3), and we had
253 shown previously that these cells had numerous Homer1-immunoreactive puncta, with
254 ~60% being associated with a Trpm8-expressing primary afferent bouton[13]. The low
255 frequency of sEPSCs is therefore not likely to result from a low density of synapses, but
256 presumably reflects a very low release probability at these synapses in these experimental
257 conditions. The lower amplitude of sEPSCs may be related to our EM observation that
258 contacts between Trpm8 afferents and densely coated lamina I projection neurons
259 typically have small synaptic specialisations (Figure 3, Figure 3–figure supplement 2).
260
261 **Targeting of cold-selective lamina I ALS neurons with the Calb1^{Cre} mouse**
262 We had previously demonstrated that lamina I projection neurons that are densely
263 innervated by Trpm8-expressing afferents are included among those of the Phox2a-
264 lineage, and contain mRNA for *Hs3st1*, one of the top differentially expressed genes for
265 ALS3. We had therefore assigned the Trpm8-innervated cells to the ALS3 cluster[13]. Calb1,
266 which encodes the calcium-binding protein calbindin, is also among the top 20 differentially
267 expressed genes for ALS3 (Figure 5–figure supplement 1A, see also Figure 1D of
268 reference[13]). However, calbindin is not restricted to the ALS3 cluster, as it is also
269 expressed by some cells in the ALS2, ALS4 and ALS5 clusters[13] (Figure 5–figure

270 supplement 1A), and by many ALS neurons in the lateral spinal nucleus (LSN)[45], most of
271 which are not derived from the Phox2a-lineage[14,46].
272 To assess the relationship between Calb1-expressing ALS neurons and those with
273 dense Trpm8 innervation, we injected an AAV coding for Cre-dependent tdTomato
274 (AAV11.Cre^{ON}.tdTomato[47]) unilaterally into the LPB of 4 Calb1^{Cre};Trpm8^{Flp};RCE:FRT mice
275 (Figure 5–figure supplement 1B). As expected from the known distribution of calbindin-
276 expressing ALS cells in the rat[45], we observed tdTomato-positive cells in lamina I (mainly
277 on the contralateral side), as well as bilaterally in the LSN and in deeper laminae (Figure
278 5A, Figure 5–figure supplement 1C-F). When we examined horizontal sections through
279 lamina I, we found that many of the tdTomato-labelled cells, were densely innervated by
280 Trpm8 afferents (Figure 5C-H), and these were located throughout the mediolateral extent
281 of the dorsal horn. The proportion of tdTomato cells with dense Trpm8 input varied
282 between 38.7-59.6% across the L2-L4 segments (Figure 5B, RM ANOVA, $p = 0.048$).
283 Interestingly, the proportion was significantly higher in L2 (59.6%) than in L4 (38.7%), (RM
284 ANOVA, Holm-Šídák's multiple comparisons test, $p = 0.0056$, $n = 4$), and this may reflect a
285 difference in the proportion of lamina I cells with dense Trpm8 innervation between
286 segments. When results across the 3 segments were pooled, the total numbers of
287 retrogradely labelled cells ranged from 133 to 170 (mean 151), while the proportions with
288 dense Trpm8 input ranged from 46.5%-54.1% (mean 50.6%). To confirm expression of
289 calbindin in lamina I projection neurons with dense Trpm8 input, we carried out
290 immunofluorescence labelling on horizontal sections from 3 Trpm8^{Flp};RCE:FRT mice that
291 had received injections of AAV9.mCherry into the LPB. We identified a total of 32
292 mCherry-positive lamina I neurons that were associated with dense GFP labelling (6-14
293 per mouse), and found that all but four of these (27/31, 87%) were calbindin-
294 immunoreactive (Figure 5–figure supplement 1G).
295 We also used the semi-intact preparation to record from tdTomato-labelled lamina I
296 neurons in spinal cords from 4 Calb1^{Cre} mice that had received injections of
297 AAV11.Cre^{ON}.tdTomato into the CVLM (Figure 5–figure supplement 1B, Figure 5–figure
298 supplement 2). We recorded from 6 retrogradely labelled neurons and found that 5 were
299 cold-selective, while one was polymodal, responding to brushing of the skin, as well as to
300 application of both hot and cold stimuli (Figure 5I,J). These cold-selective neurons
301 showed a similar time course in response to cold stimulation to those described above
302 (Figure 5–figure supplement 2C). Taken together, these findings indicate that while Calb1

303 is not restricted to cold-selective cells, many of the Calb1-expressing projection neurons in
304 lamina I belong to the cold-selective population.
305
306 **Brain projections of putative cold-selective lamina I neurons**
307 Because Calb1 is expressed by cold-selective ALS cells in lamina I, we carried out
308 anterograde tracing by injecting AAV coding for Cre-dependent expression of tdTomato
309 (AAV1.Cre^{ON}.tdTom) into the lumbar spinal cords of Calb1^{Cre} mice. Our aim was to test for
310 projections to two potential brainstem targets that receive input from the ALS[11,12] and also
311 contain many neurons that express the immediate early gene Fos in mice exposed to low
312 ambient temperatures[48-51]: the caudal part of the PAG (cPAG), and the rostral part of the
313 LPB, in particular a region that has been named PBrel (rostral to external lateral)[49]. Two
314 cortical areas are activated by skin cooling, the primary somatosensory and posterior
315 insular cortices[52]. We therefore looked for evidence of an input to the ventral posterolateral
316 (VPL) and posterior triangular (PoT) thalamic nuclei, which are thought to provide the
317 thermosensory inputs to these cortical areas in rodents[53]. Initially, we examined labelling
318 resulting from injections of AAV1.Cre^{ON}.tdTomato that were targeted on the central part of
319 the dorsal horn, either in the L3 segment, or in the L3, L4 and L5 segments, using a similar
320 approach to that which we had taken with other genotypes (Figure 6–figure supplement
321 1A,B; Table 1). Labelling patterns were consistent among the mice used in this part of the
322 study, but labelling was denser in all regions in those that had received injections into L3,
323 L4 and L5. This approach revealed that axons ascended in the dorsolateral white matter of
324 the spinal cord and gave branches to several regions on the contralateral side of the
325 brainstem, including LPB and the cPAG (Figure 6–figure supplement 1C,D). Within the
326 LPB, axonal labelling was very dense in the rostral-most part, which corresponds to
327 PBrel[49], and moderately dense in the centrolateral (PBcl) nucleus. In addition, there was
328 some labelling in other nuclei, including external lateral (PBel), dorsolateral (PBdl) and
329 internal lateral (PBil). There was dense labelling in the cPAG and in addition, labelling was
330 seen within the superior colliculus (Figure 6–figure supplement 1C). In the thalamus, there
331 was sparse labelling in the VPL, posterior (Po) and PoT nuclei contralateral to the injection
332 site, and many labelled profiles were present in the medial thalamus on both sides (Figure
333 6–figure supplement 1E). These findings were therefore consistent with the expected
334 projections of cold-selective ALS cells to PBrel, cPAG and the VPL nucleus of thalamus.
335 However, this strategy will also have labelled Calb1-expressing projection neurons in
336 other regions, including the LSN and the lateral reticulated part of lamina V (Figure 6–

337 figure supplement 1B). Consistent with this interpretation, we observed labelling in PBil
338 and the medial thalamus, both of which are known to receive input from ALS cells in the
339 deep dorsal horn[54-56], including cells belonging to the ALS4 population in lateral lamina V[5].
340 We therefore altered the injection technique by reducing the volume and injecting at a
341 more medial location (250 µm rather than 400 µm lateral to the midline). As with the
342 previous experiments, these injections were either made into the L3 segment, or into each
343 of L3, L4 and L5 (Table 1). Again, the pattern of labelling was consistent among these
344 mice, but labelling was denser in those that had received injections into L3, L4 and L5.
345 This strategy resulted in injection sites that were restricted to the medial part of the dorsal
346 horn and excluded the LSN (Fig 6A-C). Although very weak tdTomato labelling was seen
347 in the LSN in these experiments, this is likely to have arisen from transport by axons of
348 local calbindin-expressing excitatory interneurons, since many excitatory interneurons in
349 laminae I-II have axons that enter the LSN[57-59]. Importantly, no tdTomato-labelled cell
350 bodies were seen in the LSN or in the lateral reticulated part of lamina V in these cases.
351 Since these injections were likely to have included a much higher proportion of lamina I
352 neurons with dense Trpm8 innervation, we analysed the anterograde labelling in more
353 detail.
354 Axons ascended in the dorsal quadrant of the spinal cord, mainly on the contralateral
355 side (Figure 6–figure supplement 2A). Although a few collaterals arose at all segmental
356 levels examined, these were far less numerous than those originating from the
357 somatostatin-expressing ALS cells that occupy the lateral part of lamina V[5]. Ascending
358 axons lay near the ventrolateral surface of the medulla, and sent collateral branches to the
359 NTS (Figure 6D), but unlike Gpr83- and Tacr1-expressing ALS cells[5,60], these Calb1-
360 positive cells did not innervate the inferior olive. Labelling in the LPB was much more
361 restricted following medial spinal injections, compared to the central injections (Figure 6E,
362 Figure 6–figure supplement 1C,D, Figure 6–figure supplement 2B). In particular, labelling
363 in PBcl and PBil was greatly reduced, while the dense input to the PBrel was retained. The
364 input to PBrel was confirmed by immunostaining for the transcription factor Foxp2, which is
365 expressed in PBrel neurons (Fig 6G,H)[49]. There was also strong labelling in the lateral part
366 of the cPAG, (Figure 6E), but only very sparse labelling in the rostral part of the PAG
367 (Figure 6–figure supplement 2C,E). Input to both LPB and PAG was bilateral, but denser
368 on the side contralateral to the spinal injections. Labelling in the superior colliculus was
369 almost completely lost following medial spinal injections (Figure 6E). Within the thalamus,
370 the sparse labelling in VPL and Po was still present, but that in the medial thalamus was

Click here to enter text.

371 far weaker (Figure 6F,I,J). In addition, medial spinal injections resulted in labelling in the
372 PoT nucleus of the thalamus (Figure 6–figure supplement 2C,D), which is a known target
373 for lamina I ALS neurons[56,61] and is thought to convey non-noxious thermal information to
374 the posterior insular cortex[53]. Very few, if any, tdTomato-labelled axons were seen in any
375 other parts of the diencephalon[62]. High magnification scans showed that in the regions
376 targeted by tdTomato labelled axons (NTS, LPB, PAG, thalamus) these axons possessed
377 numerous varicosities, which presumably correspond to axonal boutons (Figure 6–figure
378 supplement 2F). Immunostaining for the postsynaptic density protein Homer1 revealed
379 that varicosities were often apposed to Homer1 puncta (Figure 6–figure supplement
380 2G,H), confirming that they constituted the presynaptic elements at glutamatergic
381 synapses.
382 We have previously demonstrated that although spinothalamic lamina I neurons are
383 relatively common in the rodent cervical enlargement, they are far less numerous at
384 lumbar levels, accounting for <5% of lamina I ALS neurons[46,63]. We therefore injected
385 AAV1.Cre^{ON}.tdTom into the cervical enlargement of 3 Calb1^{Cre} mice (Table 1, Figure 6–
386 figure supplement 3A,B). This resulted in far denser axonal labelling within the VPL and
387 PoT nuclei on the side contralateral to the spinal injection (Figure 6–figure supplement 3C-
388 E).
389 The differences between projection patterns of medial and central injections into the
390 lumbar enlargement provide additional information about potential targets of Calb1 cells
391 that were not located in lamina I. As noted above, the input to PBil and medial thalamus
392 seen following the central injections is likely to result at least in part from capture of cells
393 belonging to the ALS4 population in lateral lamina V[13], since we have shown that these
394 cells (targeted in a Sst^{Cre} mouse line) project to these two sites[5]. However, we found only
395 very sparse input from the Sst-expressing (ALS4) cells to the superior colliculus[5], raising
396 the possibility that input to the colliculus originates mainly from cells in the LSN, many of
397 which express Calb1. Consistent with this suggestion, Choi et al[60] observed a projection to
398 the superior colliculus from Tacr1-expressing ALS cells, and many ALS neurons in the
399 LSN express the neurokinin 1 receptor (NK1r), which is encoded by Tacr1[64-66].
400 To confirm the input to PAG from cold-selective lamina I cells, we targeted injections of
401 AAV11.Cre^{ON}.tdTomato to the caudal PAG in 3 Calb1^{Cre};Trpm8^{Flp};RCE:FRT mice. In these
402 experiments, the total numbers of retrogradely labelled (tdTomato-positive) lamina I cells
403 in the L2-L4 segments were lower than was the case for the LPB injection experiments
404 (26, 59 and 99 in the three cases), but the proportion of these cells that had dense Trpm8

Click here to enter text.

405 input was significantly higher: 84.6%, 81.4% and 77.8% ($p < 0.0001$, unpaired t-test with
406 Welch's correction; Figure 6–figure supplement 4). This indicates that, at least for
407 calbindin-expressing lamina I ALS neurons, cold-selective cells are highly enriched among
408 those that project to the caudal part of the PAG.
409 Finally, we looked for further evidence of a projection from cold-selective lamina I cells
410 to the lateral part of the thalamus by making small injections of cholera toxin B subunit
411 (CTB) in 3 Trpm8^{Flp};RCE:FRT mice. CTB was used as a retrograde tracer for these
412 experiments, because it can result in relatively small and well-defined injection sites. In all
413 3 cases, the injection was centred on the ventral posterior nucleus of thalamus, and
414 included both lateral (VPL) and medial (VPM) parts (Figure 6–figure supplement 5A-C).
415 There was some spread into Po and the ventrolateral (VL) nucleus, but none into the
416 medial thalamus and none of the injections extended as far caudally as the PoT. As
417 expected, from the low number of lamina I spinothalamic neurons at lumbar levels[46,63], few
418 (if any) retrogradely labelled cells were seen in the lumbar spinal cord in these
419 experiments (5 cells in the L4 segment of one mouse, but no cells in this segment in the
420 other two), and for this reason we focused our search on the cervical enlargement. In
421 horizontal sections through the C7 segment, we identified a large number of retrogradely
422 labelled lamina I cells in each case. Although the dendritic filling was less complete than
423 that seen with retrograde viral tracing, we were able to identify many CTB-positive cells
424 that received numerous contacts on cell bodies and dendrites from Trpm8-expressing
425 primary afferents (Figure 6–figure supplement 5D-I). In the one case in which retrogradely
426 labelled cells were detected in the L4 segment, 3 of the 5 cells were also densely coated
427 with GFP-labelled afferents (Figure 6–figure supplement 5J-L). These findings
428 demonstrate that cold-selective lamina I ALS neurons project to the lateral thalamus.
429

430 **DISCUSSION**

431 The main findings of this study are that: (1) lamina I projection neurons that are densely
432 innervated by Trpm8-expressing primary afferents correspond to the cold-selective cells
433 identified in physiological studies and receive monosynaptic input from Trpm8 afferents;
434 (2) these are captured when AAVs encoding Cre-dependent constructs are injected into
435 the brains of Calb1^{Cre} mice; and (3) axons of Calb1-positive neurons in the medial part of
436 the dorsal horn project to brain regions known to be involved in processing information
437 related to cold input, PBrel, caudal PAG, as well as the PoT and VPL nuclei of the

438 thalamus. This suggests that these sites are directly innervated by cold-selective ALS
439 neurons in lamina I.
440
441 **Lamina I ALS neurons with dense Trpm8 input are cold-selective**
442 We had previously observed that Trpm8-expressing primary afferents are closely
443 associated with the cell bodies and dendrites of a subset of ALS cells in lamina I[13]. Based
444 on their association with Homer1 puncta, we were also able to estimate that GFP-labelled
445 (Trpm8-expressing) afferents accounted for ~60% of the excitatory synapses on these
446 ALS cells. Here we directly demonstrate the presence of synapses with both electron
447 microscopy and optogenetics, and confirm our prediction[13] that these densely Trpm8-
448 innervated ALS cells correspond to the cold-selective neurons identified in previous
449 physiological studies[23-33].
450 Cold-selective lamina I projection neurons have been reported in several species,
451 including monkey[27], cat[23-26], rat[28,30] and mouse[29,31-33], and a recent *in vivo* calcium-imaging
452 study reported that they accounted for ~15% of lamina I spinoparabrachial neurons in the
453 mouse[33]. Although cold-selective lamina I projection neurons respond predominantly to
454 skin cooling, some show a weak "paradoxical" response when noxious heat is applied to
455 the skin[24,26,27,29]. We did not detect any response from cold-selective cells when hot saline
456 was applied to the skin in the experiments reported here, or in our previous study of cold-
457 selective neurons[32], and this may be because although the temperature of the hot saline
458 was 50°C, the small volume applied to the skin meant that skin temperature did not reach
459 a sufficiently high level to result in activation. It is known that some Trpm8-expressing
460 primary afferents have low levels of Trpv1[20,35,37], and some Trpm8 afferents have been
461 shown to respond weakly to noxious heat *in vivo*[35]. It has been proposed that there are two
462 different populations of Trpm8-expressing afferents: one consisting of cells that lack Trpv1
463 and respond to innocuous cooling, and the other of cells that express Trpv1, and may
464 function as "cold nociceptors"[67]. Since we found Trpv1-immunoreactivity in around a
465 quarter of GFP-labelled dorsal root ganglion cells, it is likely that both populations are
466 included amongst the GFP-expressing cells in the Trpm8^{Flp};RCE:FRT mice. However, we
467 were unable to detect Trpv1-immunoreactivity in the central terminals of any GFP-positive
468 axons (presumably reflecting the low level of Trpv1 expressed by these cells), and we
469 therefore do not know whether the Trpm8-positive axons synapsing on cold-selective
470 lamina I ALS neurons include those that express Trpv1. However, if this is the case, it is

471 likely to explain the weak response to noxious heat reported for some cold-selective
472 projection neurons[24,26,27,29].
473
474 **Direct and indirect input from Trpm8 afferents to cold-selective ALS neurons**
475 Our findings clearly demonstrate a major direct (monosynaptic) input from Trpm8-
476 expressing primary afferents to cold-selective lamina I projection neurons. We had
477 previously estimated that a mean of 62% of the Homer1 puncta (which correspond to
478 excitatory synapses) on cell bodies and dendrites of these cells were associated with
479 GFP-positive boutons in Trpm8^{Flp}:RCE:FRT mice[13]. However, we show here that this line
480 only labels ~83% of Trpm8-expressing primary afferent neurons with GFP. If this
481 proportion applies equally to Trpm8 afferents that synapse on cold-selective ALS cells,
482 then Trpm8 afferents would give rise to ~75% of the excitatory synapses on these cells.
483 Lee et al[34] recently proposed that there is a dedicated population of superficial dorsal
484 horn excitatory interneurons that express the thyrotropin releasing hormone receptor (Trhr)
485 and form a disynaptic link between Trpm8 afferents and cold-selective lamina I projection
486 neurons. Interestingly, in their initial experiments, they ablated or silenced calbindin-
487 expressing dorsal horn neurons and found that this reduced behavioural responses to skin
488 cooling. Although they interpreted this as resulting from loss of function of calbindin-
489 expressing excitatory interneurons, our findings indicate that they are also likely to have
490 ablated or silenced calbindin-expressing cold-selective lamina I ALS neurons. This could
491 therefore have made a major contribution to the reduced sensitivity to skin cooling. Having
492 obtained evidence that cold-responsive Calb1+ neurons in the dorsal horn often co-
493 expressed Trhr, Lee et al generated a Trhr^{Cre} mouse line and used spinal injection of AAVs
494 coding for Cre-dependent constructs, or a genetic intersectional approach, to target Trhr-
495 expressing spinal neurons[34]. They ablated these cells and found that this selectively
496 reduced responses to skin cooling. They also reported that when AAV.Cre^{ON}.YFP was
497 injected intraspinally in Trhr^{Cre} mice, there was no axonal labelling in the brain, suggesting
498 that Trhr-expressing dorsal horn neurons were exclusively interneurons. However, this
499 observation is not consistent with our transcriptomic dataset[13], which reveals Trhr
500 expression in some Phox2a-derived ALS neurons, including some of those in the ALS3
501 cluster (Figure 7-figure supplement 1). It is therefore not clear why a brain projection from
502 Trhr cells was not detected by Lee et al, although it is possible that the survival time
503 allowed for anterograde transport of YFP (reported as 2-3 weeks) was not sufficient. Lee
504 et al[34] also reported that the cold-selective ALS neurons were marked by expression of the

505 calcitonin receptor-like receptor (encoded by the *Calcrl* gene). However, this is unlikely to
506 be a specific marker, as our data show expression of Calcrl among several populations of
507 Phox2a-derived ALS neurons[13] (Figure 7-figure supplement 1), and it has been reported
508 that Calcrl is also expressed by spinoparabrachial neurons that are required for
509 mechanical itch[68].
510 While our findings do not exclude the possibility that there is a specific population of
511 interneurons that link Trpm8-expressing primary afferents to cold-selective ALS neurons in
512 lamina I, they clearly demonstrate a substantial direct (monosynaptic) input from Trpm8
513 afferents to cold-selective lamina I projection neurons, and indicate the need for caution in
514 relying on the specificity of individual genetic markers to define neurons and circuits in the
515 dorsal horn.
516
517 **Brain targets of cold-selective ALS cells**
518 At present there is no known molecular marker that could be used to target cold-
519 selective lamina I ALS cells exclusively. We chose calbindin because *Calb1* is among the
520 top differentially expressed genes in the ALS3 cluster[13], and there is a well-established
521 knock-in Cre line available[69]. Importantly, our transcriptomic analysis[13] was restricted to
522 projection neurons derived from the Phox2a lineage[14], which excludes most ALS cells in
523 the LSN and ~40% of those in lamina I[14,46]. Menetrey et al[45] had demonstrated that
524 calbindin-immunoreactive spinoparabrachial neurons in rat were located in lamina I, the
525 LSN and lateral lamina V, with scattered cells around the central canal, and this closely
526 matches the distribution of cells labelled when AAV11.Cre^{ON}.tdTomato was injected into
527 the LPB of Calb1^{Cre} mice. For anterograde tracing, we were able to exclude LSN and
528 lateral lamina V ALS cells by injecting smaller volumes into the medial part of the dorsal
529 horn, and this was confirmed by the lack of axonal labelling in regions known to receive
530 input from these cells (e.g., PBil and medial thalamus)[5,54,56]. However, although our medial
531 injections preferentially captured cold-selective lamina I ALS neurons they will also have
532 labelled cells that are not cold-selective, including some lamina I cells in the ALS2 cluster[13]
533 and potentially some of those that are not derived from the Phox2a lineage[46]. We therefore
534 focused our analysis on brain regions known to be involved in cold sensing, and tested
535 whether these received input from the Calb1-positive ALS cells.
536 Among the ALS projection targets that contain cells responding to cold, we were able to
537 show a dense input to the rostral part of the LPB and to the cPAG. Two studies have
538 mapped neurons in LPB that express Fos in mice exposed to low ambient

539 temperatures[49,50], and both found that Fos-positive cells were concentrated in the rostral
540 part of the LPB, corresponding to a level ~4.9 mm caudal to bregma (or 1.1 mm caudal to
541 the interaural line)[62]. Yang et al[50] identified the region containing Fos+ cells as part of the
542 external lateral (PBel) nucleus, while Geerling et al[49] defined it as the PBrel, and showed
543 that this area could be recognised by the expression of Foxp2. Yang et al[50] reported that
544 cold-activated cells in this region projected to the preoptic area (POA), which is known to
545 form part of a cold-defence circuit[70], as well as to the dorsomedial hypothalamus (DMH).
546 They also showed that parabrachial neurons targeting DMH promoted activation of brown
547 adipose tissue, suggesting a role for both of these hypothalamic areas in maintenance of
548 body temperature in cold conditions. The cold-selective lamina I ALS cells are therefore
549 likely to provide an important source of input to POA and DMH via their projection to PBrel,
550 thus forming part of the afferent limb of a cold defence pathway (Figure 7).
551 Neurons in the cPAG show increased Fos expression in rats exposed to low ambient
552 temperatures[48], and this region receives an input from cold-activated cells in the
553 hypothalamus[51]. Our results demonstrate that Calb1-positive neurons in the dorsal horn
554 also provide a dense input to the cPAG. Although we cannot be certain that this originates
555 from the cold-selective ALS neurons, there are two lines of evidence to support this
556 suggestion. First, Li et al[71] demonstrated innervation of mouse lamina I spino-PAG
557 neurons by Trpm8-expressing primary afferents, and second, we found that ~80% of
558 Calb1 neurons retrogradely labelled from cPAG received dense Trpm8 input. Consistent
559 with this interpretation, we had previously reported that rat lamina I neurons retrogradely
560 labelled from the PAG seldom showed strong expression of the NK1r, unlike those labelled
561 from the LPB or CVLM[72], and cold-selective lamina I neurons have been shown to respond
562 weakly, if at all, to substance P, the main ligand for this receptor[32]. These findings suggest
563 that the cold-selective lamina I neurons provide a direct input to cPAG, which presumably
564 contributes to the responsiveness of neurons in this region to cooling[48]. Activation of
565 neurons in the cPAG results in brown adipose tissue thermogenesis[73], suggesting a role in
566 maintenance of body temperature in cold conditions (Figure 7).
567 Our CTB injections into the lateral thalamus were centred on the ventral posterior
568 nucleus, with a varying degree of spread into Po, which was also found to receive input
569 from Calb1-positive ALS neurons. It is not possible to determine precisely the region(s)
570 from which retrograde transport would occur, but since we identified lamina I cells in the
571 C7 segment (and in one case also in the L4 segment) with relatively strong CTB labelling
572 that were associated with GFP-labelled axons, these are likely to have projected to the

Click here to enter text.

573 core of the injection site, i.e. the ventral posterior nucleus. As noted above, spinothalamic
574 lamina I neurons are infrequent in the rodent lumbar enlargement[46,63], and this presumably
575 accounts for the very sparse labelling in VPL that we saw following injections of
576 AAV1.Cre^{ON}.tdTomato into the lumbar spinal cord, compared to that seen after cervical
577 injections. However, our findings from the retrograde tracing experiments suggest that
578 cold-selective cells project to VPL, and this is consistent with the demonstration of input
579 from cervical lamina I neurons to VPL in the rat[56]. In addtion, we identified an input to the
580 PoT nucleus of thalamus, which projects to the posterior insular cortex[53]. Together, the
581 input from cold-selective lamina I ALS cells to PoT and VPL is likely to contribute to the
582 perception of cold stimuli applied to the skin through the projections of these thalamic
583 nuclei to the posterior insular and somatosensory cortices[53] (Figure 7).
584
585
586 **MATERIALS AND METHODS**
587
588 **Key resources table**

Reagent or resource	Source	Identifier
Mouse lines		
Trpm8^{Flp}	Dr Mark Hoon	N/A
B6.Cg-Gt(ROSA)26Sor$^{tm9(CAG\text{-}tdTomato)Hze}$/J (Ai9)	Prof. Hongkui Zheng; available from The Jackson Laboratory, ME, USA	Cat#: 007909 RRID: IMSR_JAX:007909
Phox2a::Cre	Prof Artur Kania	N/A
STOCK *Gt(ROSA)26Sor*$^{tm1.2(CAG\text{-}EGFP)Fsh}$/Mmjax (RCE:FRT)	The Jackson Laboratory, ME, USA	Cat#: 032038 RRID:MMRRC_032038-JAX
B6;129S-*Calb1*$^{tm2.1(cre)Hze}$/J (Calb1^{Cre})	The Jackson Laboratory, ME, USA	Cat#: 028532 RRID:IMSR_JAX:028532
AAV constructs		
pENN.AAV.CB7.CI.mCherry.WPRE.RBG (AAV9.mCherry)	Penn Vector Core, PA, USA; available from Addgene, MA, USA	Cat#: 105544-AAV9 RRID:Addgene_105544
pssAAV-2-CAG-EGFP_Cre-WPRE-SV40p(A) (AAV9.EGFP_Cre)	Viral Vector Facility, University of Zurich, Switzerland	Cat#: v25-9
pssAAV-2-CAG-dlox-tdTomato(rev)-dlox-WPRE-bGHp(A) (AAV1.Cre^{ON}.tdTomato)	Viral Vector Facility, University of Zurich, Switzerland	Cat#: v167-1
AAV11.CAG.Cre^{ON}.tdTomato (AAV11.Cre^{ON}.tdTomato)	BrainCase Biotechnology Co Ltd, Wuhan, China	Cat#: BC-0870
AAV.PHP.S.Flp^{ON}.ChR2_YFP	Viral Vector Facility, University of Zurich, Switzerland	Cat#: v237-PHP.S
AAV11.CAG.tdTomato (AAV11.tdTomato)	BrainCase Biotechnology Co Ltd, Wuhan, China	Cat#: BC-0868

Antibodies		
Chicken anti-GFP (1:1000)	Abcam plc	Cat#: ab13970 RRID: AB_300798
Rabbit anti-GFP (1:1000)	M Watanabe	RRID:AB_2571573
Rat anti-mCherry (1:1000)	Thermo Fisher Scientific	Cat#: M11217 RRID: AB_2536611
Guinea pig anti-NeuN (1:1000)	Synaptic Systems	Cat#: 266 004 RRID:AB_2619988
Rabbit anti-NeuN-Alexa Fluor® 647 (1:1000)	Abcam plc	Cat#: EPR12763 RRID:AB_2532109
Rat anti-substance P (1:200)	Oxford biotechnology	Cat#: OBT06435
Rabbit anti-substance P (1:1000)	Peninsula	Cat#: T-4107 RRID:AB_518630
Rabbit anti-TRPV1 (1:1000)	Synaptic Systems	Cat#: 444 013 RRID:AB_2864792
Sheep anti-CGRP (1:2000)	Enzo	Cat#: BML-CA1137 RRID:AB_2243859
Rabbit anti-somatostatin (1:500)	Peninsula	Cat#: T-4103 RRID:AB_518614
Guinea pig anti-VGLUT3 (1:100)	M Watanabe	RRID:AB_2571856
Sheep anti-Foxp2 (1:500)	Biotechne	Cat#: AF5647 RRID:AB_2107133
Goat anti-cholera toxin B subunit (1:2000 for immunofluorescence; 1:100,000 for immunoperoxidase)	List Biological	Cat#: 703 RRID:AB_10013220
Goat anti-Homer1 (1:500)	M Watanabe	RRID:AB_2631104
Rabbit anti-calbindin (1:1000)	Swant	Cat#: CB38 RRID:AB_10000340
Alexa Fluor™ Plus 405 Donkey anti-Rabbit IgG (1:500)	Thermo-Fisher Scientific	Cat#: A48258 RRID: AB_2890547
Alexa Fluor® 488 Donkey Anti-Chicken IgY (1:500)	Jackson ImmunoResearch	Cat#: 703-545-155 RRID: AB_2340375
Alexa Fluor® 488 Donkey anti-Goat IgG (1:500)	Jackson ImmunoResearch	Cat#: 705-545-147 RRID: AB_2336933
Alexa Fluor® 488 Donkey Anti-Rabbit IgG (1:500)	Jackson ImmunoResearch	Cat#: 711-545-152 RRID: AB_2313584
Alexa Fluor™ Plus 488 Donkey anti-Rabbit IgG (1:500)	Thermo-Fisher Scientific	Cat#: A32790 RRID: AB_2762833
Rhodamine Red™-X Donkey Anti-Guinea pig IgG (1:100)	Jackson ImmunoResearch	Cat#: 706-295-148 RRID: AB_2340468
Rhodamine Red™-X Donkey Anti-Rabbit IgG (1:100)	Jackson ImmunoResearch	Cat#: 711-295-152 RRID: AB_2340613
Rhodamine Red™-X Donkey Anti-Rat IgG (1:100)	Jackson ImmunoResearch	Cat#: 712-295-153 RRID: AB_2340676
Alexa Fluor™ Plus 555 Donkey anti-Rat IgG (1:500)	Thermo-Fisher Scientific	Cat#: A48270 RRID:AB_2896336
Alexa Fluor™ Plus 555 Donkey anti-Goat IgG (1:500)	Thermo-Fisher Scientific	Cat#: A32816 RRID:AB_2762839

Click here to enter text.

Alexa Fluor® 647 Donkey Anti-Rabbit IgG (1:500)	Jackson ImmunoResearch	Cat#: 711-605-152 RRID:AB_2492288
Alexa Fluor® 647 Donkey Anti-Goat IgG (1:500)	Jackson ImmunoResearch	Cat#: 705-605-147 RRID: AB_2340437
Alexa Fluor® 647 Donkey Anti-Guinea pig IgG (1:500)	Jackson ImmunoResearch	Cat#: 706-605-148 RRID: AB_2340476
Biotin-SP Donkey Anti-Goat IgG (1:500)	Jackson ImmunoResearch	Cat#: 705-065-147 RRID: AB_2340397
Biotin-SP Donkey Anti-Guinea pig IgG (1:500)	Jackson ImmunoResearch	Cat#: 706-065-148 RRID: AB_2340451
Biotin-SP Donkey Anti-Rabbit IgG (1:500)	Jackson ImmunoResearch	Cat#: 711-065-152 RRID: AB_2340593
Avidin conjugates		
Extravidin-Peroxidase	Sigma-Aldrich	Cat#: E2886 RRID:AB_2620165
Streptavidin-Pacific Blue	Life Technologies	Cat#: S11222
HCR probe		
Mm-Trpm8 v3.0	Molecular Instruments	
Chemicals		
Cholera toxin B subunit	Sigma-Aldrich	Cat#: C9972
DAPI	Sigma-Aldrich	Cat#: D9542
Sodium borohydride	Sigma-Aldrich	Cat#: 452882
3,3'-Diaminobenzidine	Revvity	Cat#: NEL938001EA
Hydrogen peroxide	Sigma-Aldrich	Cat#: H1009
Osmium tetroxide	Agar Scientific	Cat#: R1016
Uranyl acetate	Agar Scientific	Cat#: R1260A
Lead citrate	Agar Scientific	Cat#: R1210
Software		
Neurolucida	MBF Bioscience	https://www.mbfbioscience.com/neurolucida RRID: SCR_001775
Neurolucida Explorer	MBF Bioscience	https://www.mbfbioscience.com/neurolucida-explorer RRID: SCR_017348
pClamp	Molecular Devices	https://www.moleculardevices.com/products/axon-patch-clamp-system/acquisition-and-analysis-software/pclamp-software-suite#gref RRID: SCR_011323
Easy Electrophysiology	Easy Electrophysiology LTD	https://www.easyelectrophysiology.com
Zen Black	Carl Zeiss	https://www.zeiss.com/microscopy/int/products/microscope-software/zen.html RRID: SCR_018163
Prism	GraphPad Software	https://www.graphpad.com/scientific-software/prism/

Click here to enter text.

		RRID: SCR_002798
Photoshop CS6	Adobe Systems Incorporated	https://www.adobe.com/
Xara Xtreme v2.0	Xara Group Ltd	https://www.xara.com/
Inkscape	Software Freedom Conservancy	https://inkscape.org/

589 **Experimental Model and Subject Details**

590 All experiments were approved by the Ethical Review Process Applications Panel of the
591 University of Glasgow, and were carried out in accordance with the UK Animals (Scientific
592 Procedures) Act 1986 and ARRIVE guidelines. The following transgenic mouse lines were
593 used in this study: the BAC transgenic Phox2a::Cre line, which expresses Cre
594 recombinase under control of the Phox2a promoter[14]; the Ai9 Cre reporter line, in which a
595 loxP-flanked STOP cassette prevents CAG promoter-driven transcription of tdTomato[69];
596 the Trpm8^{Flp} line, in which 2A-linked FlpO recombinase is fused with the last codon (and
597 replaces the stop codon) of the *Trpm8* gene[13]; the RCE:FRT line, which carries the R26R
598 CAG-boosted EGFP reporter allele with a FRT-flanked STOP cassette upstream of the
599 EGFP gene[74]; and the Calb1^{Cre} line which has an IRES2 sequence and a Cre
600 recombinase gene inserted downstream of the translational STOP codon of the calbindin 1
601 gene[75]. Further details of these lines can be found in the Key Resources table. The
602 following crosses were generated by cross-breeding these lines: Trpm8^{Flp};RCE:FRT mice,
603 which were used for anatomical analysis of Trpm8-expressing DRG cells, for
604 electrophysiological experiments, and for retrograde tracing of spinothalamic neurons;
605 Trpm8^{Flp};RCE:FRT;Ai9 mice, which were used for some electrophysiological experiments;
606 Trpm8^{Flp};RCE:FRT;Phox2a::Cre;Ai9 mice, which were used for the combined confocal and
607 electron microscopic analysis; and Calb1^{Cre};Trpm8^{Flp};RCE:FRT mice, which were used to
608 determine the proportion of retrogradely labelled Calb1-expressing cells that received
609 dense Trpm8 input.

610 Perfusion fixation was performed while mice were deeply anaesthetised with
611 pentobarbitone (20 mg i.p.). A brief rinse with Ringer's solution was followed by perfusion
612 with ~250 ml of fixative. In all cases apart from those used for combined confocal/electron
613 microscopy the fixative consisted of 4% freshly depolymerised formaldehyde in phosphate
614 buffer (PB). Spinal cords and brains were dissected and stored in the same fixative for 2
615 hours, before being transferred to 30% sucrose in PB.

616 Dorsal root ganglia for FISH were obtained from Trpm8^{Flp};RCE:FRT mice, which had
617 been killed with an overdose of pentobarbital (40 mg i.p.) and perfused with cold
618 phosphate buffered saline (PBS). The ganglia were fixed in 4% formaldehyde for 2 hours.

619 Mice of both sexes, aged 4-14 weeks and weighing between 13 and 25 g at the start of
620 any surgical procedures were used in the study.
621
622 **Fluorescent *in situ* hybridisation, immunohistochemistry and imaging**
623 FISH was performed on intact lumbar dorsal root ganglia from Trpm8^{Flp};RCE:FRT mice
624 using HCR RNA-FISH v3.0 reagents. Tissues were dehydrated in graded ethanol
625 solutions, followed by rinsing in PBS. Hybridisation and amplification were performed with
626 a probe against mouse *Trpm8* mRNA and hairpins conjugated to Alexa Fluor 546 (HCR
627 v3.0, Molecular Instruments, Inc.) according to the manufacturer's instructions. Tissues
628 were mounted using antifade mounting medium and stored at -20°C.
629 Sections of brain, spinal cord and dorsal root ganglia for immunohistochemical
630 processing were cut on either a vibrating blade microtome (Leica VT1000 or VT1200) or a
631 cryostat (Leica CM1950). Section thickness was 50 µm for brain and 60 µm for spinal cord
632 and dorsal root ganglia. Multiple-label immunofluorescence microscopy was carried out as
633 described previously[5,59,76]. Reactions were performed on free-floating sections, and the
634 sources and concentrations of antibodies are listed in the Key Resources Table. Sections
635 were incubated for 1-3 days at 4°C or room temperature in primary antibodies diluted in
636 PBS that contained 0.3M NaCl, 0.3% Triton X-100 (except for tissue processed by the
637 confocal/EM method) and 5% normal donkey serum. After rinsing they were incubated for
638 2-18 hours in appropriate species-specific secondary antibodies that were raised in
639 donkey and conjugated to Alexa Fluor Plus 405, Alexa Fluor 488, Alexa Fluor Plus 488,
640 Alexa Fluor Plus 555, Alexa Fluor 647 or Rhodamine Red, in the same diluent. Following
641 the reaction, sections were mounted with anti-fade medium and stored at -20°C.
642 Tissue sections and dorsal root ganglia that had undergone immunofluorescence
643 labelling or FISH were scanned with either a Zeiss LSM710 confocal microscope with
644 Argon multi-line, 405 nm diode, 561 nm solid state and 633 nm HeNe lasers, or with a
645 Zeiss LSM900 Airyscan confocal microscope with 405, 488, 561 and 640 nm diode lasers.
646 Confocal image stacks were obtained through a 20x dry lens (numerical aperture, NA,
647 0.8), or through 40x (NA 1.3) or 63x (NA 1.4) oil immersion lenses with the confocal
648 aperture set to 1 Airy unit or less.
649 The method for combining confocal and electron microscopy was the same as that
650 described previously[77]. Two Trpm8^{Flp};RCE:FRT;Phox2a::Cre;Ai9 mice were perfused with
651 fixative that contained 0.5% glutaraldehyde and 4% formaldehyde. Horizontal sections of
652 spinal cord were obtained from lumbar segments, and these were treated with 50%

653 ethanol for 30 mins, to enhance antibody penetration, and then with 1% sodium
654 borohydride for 30 mins to quench unbound aldehyde sites. After rinsing, they were
655 incubated for 3 days in primary antibodies against GFP (raised in rabbit) and mCherry
656 (raised in rat), and then overnight in a mixture of secondary antibodies: donkey anti-rabbit
657 conjugated to Alexa Fluor 488, donkey anti-rabbit conjugated to biotin and donkey anti-rat
658 conjugated to Rhodamine Red. Note that the anti-mCherry antibody recognises tdTomato.
659 The antibody diluent consisted of PBS that contained 0.3M NaCl and 5% normal donkey
660 serum. They were then incubated in avidin conjugated to horseradish peroxidase (HRP)
661 and mounted on slides with anti-fade medium. Sections were viewed with a confocal
662 microscope, and regions that contained tdTomato-positive cells that were densely coated
663 with GFP-labelled axons were selected. These were scanned with the confocal
664 microscope to generate z-series through the cell bodies and dendritic trees of the neurons.
665 The sections were then removed from the slides, rinsed in PBS and then PB, processed
666 with 3,3'-diaminobenzidine (DAB) and H_2O_2 to reveal peroxidase-labelled (Trpm8-positive)
667 axons, osmicated, stained with uranyl acetate, dehydrated and flat-embedded in Durcupan
668 resin between acetate sheets[77]. Series of ultrathin sections (silver interference colour)
669 were cut with a diamond knife and collected on Formvar-coated slot grids. These were
670 further stained with lead citrate and viewed with either a Philips CM100 or Jeol JEM-
671 1400Flash electron microscope.
672
673 **Intracranial and intraspinal injections**
674 All surgical procedures involving intraspinal and/or intracranial injections were
675 performed while the mice were anaesthetised with isoflurane (1-2%), and all animals
676 received perioperative analgesia (buprenorphine 0.1 mg/kg and carprofen 10 mg/kg, s.c.).
677 For both types of injection, the mice were placed in a stereotaxic frame.
678 For intracranial injections, lidocaine (10 mg/kg, s.c.) was injected into the skin over the
679 skull, which was then incised. Burr holes were drilled to allow targeting at the following co-
680 ordinates (CVLM: 1.1-1.3 mm lateral to midline, 3.5 mm caudal to lambdoid suture, 3.3-3.7
681 mm below brain surface; LPB: 1.1 mm lateral to the midline, 0.35 mm caudal to lambdoid
682 suture or 4.5 mm caudal to bregma, 3.0 mm below brain surface, PAG: 0.4 mm lateral to
683 midline, 0.4 mm caudal to the interaural line, 3.1 mm below brain surface; VPL: 1.6-1.7
684 lateral to the midline, 0.79-1.11 caudal to bregma, 3.4 mm below brain surface). Injections
685 were made through glass micropipettes (outer tip diameter ~60 μm) attached to a Harvard
686 Pump 11 Elite (for AAV injections) or a PV 800 Pneumatic Picopump (WPI; for CTB

687 injections). For optogenetic experiments, Trpm8^{Flp}RCE:FRT mice that had received
688 intraperitoneal injections of AAV.PHP.S.Flp^{ON}.ChR2_YFP (see below) were injected with
689 AAV11.tdTomato (2.5×10^{9} GC in 500 nl) into the LPB or CVLM. Brain injections for the
690 electrophysiological experiments in which the semi-intact preparation was used to record
691 from cells with or without dense Trpm8 input consisted of AAV9.mCherry (7.5×10^{8}-
692 1.2×10^{10} GC in 500 nl) injected into the LPB or CVLM of Trpm8^{Flp};RCE:FRT mice, or
693 AAV9.Cre_GFP (3.5×10^{9} GC in 500 nl) injected into the CVLM of a Trpm8^{Flp};RCE:FRT;Ai9
694 mouse. For anatomical experiments involving Calb1^{Cre};Trpm8^{Flp};RCE:FRT mice
695 AAV11.Cre^{ON}.tdTomato was injected into LPB (2×10^{9} GC in 400 nl) or PAG (1×10^{9} GC in
696 200 nl). For the immunohistochemical analysis of calbindin expression in Trpm8-
697 innervated neurons, Trpm8^{Flp};RCE:FRT mice received injections of AAV9.mCherry
698 (7.5×10^{8}-1.2×10^{10} GC in 500 nl) into the LPB. For electrophysiological recording of Calb1-
699 expressing neurons in the semi-intact preparation, 4 Calb1^{Cre} mice were injected with
700 AAV11.Cre^{ON}.tdTomato into the CVLM (2×10^{9} GC in 400 nl). Injections into the lateral
701 thalamus consisted of 100 nl of 1% CTB. Micropipettes were left in place for ~5 mins after
702 the injection to limit leakage up the track. For electrophysiological experiments mice were
703 allowed to recover for between 9 and 22 days (see below for further details). For
704 anatomical experiments, survival times were 3 days for CTB injections and 12-16 days for
705 AAV injections and these were followed by perfusion fixation, as described above.
706 For intraspinal injections in lumbar spinal cord the T12 and L1 vertebrae were exposed
707 and clamped. Injections were made through glass micropipettes (outer tip diameter ~60
708 µm) attached to a 10 µL Hamilton syringe, on the right side of the spinal cord into either
709 the L3 segment, or the L3, L4 and L5 segments. Injections into L3 and L5 were made
710 through the intervertebral spaces on either side of the T13 vertebra, while those into L4
711 were made through a small hole drilled in the lamina of the T13 vertebra. In initial
712 experiments we used a similar strategy to that described in previous papers[5,64], and these
713 are referred to as “central” injections. We subsequently modified the technique in order to
714 restrict injection sites to the medial part of the dorsal horn and exclude the LSN, and we
715 refer to these as “medial” injections. For cervical injections, the head was held in place
716 with ear-bars and the T2 spine was clamped. Injections were made (as described above)
717 in the intervertebral space between the C6 and C7 vertebrae. The mice survived between
718 26 and 57 days and were then deeply anaesthetised and perfused with fixative as
719 described above (for further details see Table 1).
720

721 **Image analysis**

722 Lamina I ALS neurons that received numerous contacts from GFP-positive (Trpm8-
723 expressing) primary afferents were identified in several parts of this study, either following
724 retrograde labelling or through expression of tdTomato (in crosses that involved
725 Phox2a::Cre and Ai9). The cells could be readily identified by the close association of
726 GFP-labelled axons with their dendrites, which received multiple contacts from GFP-
727 positive boutons. In most cases the cell bodies were also associated with numerous GFP-
728 labelled boutons, and these sometimes completely surrounded the cell body[13].

729 All quantitative image analyses were performed with Neurolucida for Confocal software
730 (MBF Bioscience, Williston, VT, USA).

731 To determine the proportion of DRG neurons that were labelled with GFP in
732 Trpm8^{Flp};RCE:FRT mice we scanned 3 or 4 sections immunostained to reveal GFP and
733 NeuN, and counterstained with DAPI from the L4 dorsal root ganglia from each of 3 mice
734 (1 male, 2 female) with a confocal microscope. Z-stacks that included the complete cross-
735 sectional area of the ganglion were analysed using a modified disector method[78].
736 Reference and look-up sections were set 10 μm apart, and all intervening sections were
737 examined to reveal any neurons that might have been located between these two levels.
738 Initially we viewed the NeuN and DAPI channels, and in this way, we identified all neurons
739 (between 904 and 1383 per mouse) for which the top surface of the nucleus was located
740 between reference and look-up section. We then revealed the channel for GFP and
741 counted any of the sampled neurons that were GFP-immunoreactive.

742 For the comparison of *Trpm8* mRNA and GFP dorsal root ganglia from 3
743 Trpm8^{Flp};RCE:FRT mice (1 male, 2 female) that had been reacted as described above
744 were scanned with a confocal microscope to generate z-series through the entire volume
745 of the ganglion. Initially, both fluorescent channels (GFP and Alexa Fluor 546) were
746 combined such that any cell with either GFP or *Trpm8* mRNA was visible. For all of these
747 cells (between 155-209 per mouse), the cell size was determined by drawing an outline of
748 the cell at its maximum point and converting cross-sectional area to diameter by assuming
749 a circular shape. The two fluorescent channels were then separated, and for each cell the
750 presence of GFP and/or *Trpm8* mRNA was determined.

751 Because we found a relatively limited range of sizes for GFP/*Trpm8*-positive cells (see
752 Figure 1C) we did not use a stereological method for analysing co-localisation with other
753 neurochemical markers. We scanned sections of dorsal root ganglia immunoreacted to
754 reveal GFP together with: (1) VGLUT3, (2) Trpv1, (3) CGRP and substance P, or (4)

Click here to enter text.

755 somatostatin. In each case tissue from 3 mice (either 2 male and 1 female, or 1 male and
756 2 female) was used, and z-stacks covering the entire cross-sectional area of the ganglion
757 were analysed. Initially the GFP channel was viewed and the locations of all labelled cells
758 were marked (between 126 and 350 per mouse for each reaction). The other channel(s)
759 was/were then examined and the presence or absence of the other marker(s) was noted.
760 To determine the proportion of retrogradely labelled lamina I neurons that had dense
761 input from Trpm8-expressing afferents in the Calb1^{Cre};Trpm8^{Flp};RCE:FRT mice injected
762 with AAV11.Cre^{ON}.tdTomato into either LPB (4 mice, 2 male and 2 female) or PAG (3
763 mice, 1 male, 2 female), we examined horizontal sections cut through the L2, L3 and L4
764 segments. These had been immunostained to reveal GFP and tdTomato, and were
765 scanned with a confocal microscope. The resulting z-stacks were viewed with Neurolucida
766 software, initially with only the tdTomato channel visible, and the locations of retrogradely
767 labelled lamina I neurons were recorded (between 32 and 81 cells per segment in each
768 animal for the experiments involving LPB injections). For the experiments involving PAG
769 injections, numbers of retrogradely labelled neurons were much lower, and results from
770 the 3 segments were pooled for each animal (between 26 and 99 cells per mouse). The
771 GFP channel was then viewed, and cells that received dense Trpm8 input were identified.
772 The L5 segments of the 4 Calb1^{Cre};Trpm8^{Flp};RCE:FRT mice that had received injections
773 into LPB mice were cut transversely and the locations of tdTomato-labelled cell bodies on
774 between 8 and 10 individual sections were identified. These were then morphed onto a
775 standard outline of the L5 segment in Inkscape, resulting in single scalable vector graphics
776 files for each mouse.
777 To test whether cold-selective cells were included among those projecting to the lateral
778 thalamus, we examined horizontal sections from the L4 and C7 segments of 3
779 Trpm8^{Flp};RCE:FRT mice (2 male, 1 female) that had received CTB injections into the
780 lateral thalamus. Sections were immunoreacted to reveal CTB and GFP and scanned with
781 a confocal microscope. We then searched for CTB-labelled cells that were associated with
782 numerous GFP-positive axons.
783 For anterograde tracing following intraspinal injections of AAV1.Cre^{ON}.tdTomato in
784 Calb1^{Cre} mice, sections were first viewed with a fluorescence microscope (Zeiss Axioscope
785 5) and selected sections were scanned with a confocal microscope. Identification of brain
786 regions that contained tdTomato-labelled axons was generally based on the atlas of
787 Franklin and Paxinos[62], apart from the LPB. For this, we used the same terminology as in

our previous paper[64], and identified the PBrel nucleus based on the findings of Geerling et al[49].

Whole spinal cord preparation

The whole spinal cord preparation was made as described previously with minor modifications[44]. Animals were anaesthetised with isoflurane, followed by a lethal dose of pentobarbital, and then quickly perfused with oxygenated sucrose-based artificial cerebrospinal fluid (ACSF; in mM; 3.0 KCl, 1.2 NaH2PO4, 0.5 CaCl2, 7.0 MgCl2, 26.0 NaHCO3, 15.0 glucose, 251.6 sucrose, 1.0 Na ascorbate, and 1.0 Na pyruvate). Immediately after perfusion, the back skin was incised and the spinal cord was quickly excised and placed into a sucrose-based ACSF. Dura and pia-arachnoid membranes were removed. The spinal cord was pinned into a chamber wall made from Sylgard.The spinal cord was perfused with oxygenated normal ACSF (in mM; 125.8 NaCl, 3.0 KCl, 1.2 NaH_2PO_4, 2.4 $CaCl_2$, 1.3 $MgCl_2$, 26.0 $NaHCO_3$, and 15.0 glucose) at 25˚C.

Semi-intact somatosensory preparation

The semi-intact somatosensory preparation was made as described previously[31,32] with minor modifications. Mice were anaesthetised with isoflurane, followed by a lethal dose of pentobarbital, and then quickly perfused with oxygenated sucrose-based artificial cerebrospinal fluid (ACSF; in mM; 3.0 KCl, 1.2 NaH_2PO_4, 0.5 $CaCl_2$, 7.0 $MgCl_2$, 26.0 $NaHCO_3$, 15.0 glucose, 251.6 sucrose, 1.0 Na ascorbate, and 1.0 Na pyruvate). The back skin was incised, and the spinal cord was exposed by dorsal laminectomy. The right hindlimb and the right side of the trunk with the spinal cord were excised and transferred to the dissection/recording chamber, and tissues were submerged in the oxygenated sucrose-based ACSF. The right hind paw skin, saphenous nerve, and femoral cutaneous nerve were carefully isolated from the surrounding tissues. Only the L2 and L3 ganglia on the right side were left attached to the spine. All dorsal roots except L2 and L3, dural and pial membranes were carefully removed. The spinal cord was pinned onto a Sylgard chamber with the right dorsal horn facing upward. The tissued was perfused with oxygenated normal ACSF (in mM; 125.8 NaCl, 3.0 KCl, 1.2 NaH_2PO_4, 2.4 $CaCl_2$, 1.3 $MgCl_2$, 26.0 $NaHCO_3$, and 15.0 glucose) at 25˚C. Recordings were performed for up to 4 hours after dissection. The hindpaw skin was also at a temperature of 25˚C. At this temperature Trpm8 afferents will have been active, but are likely to have adapted over the

821 course of the experiment. In addition, the conduction velocity of their axons will have been
822 lower than in the *in vivo* state.
823
824 **Patch-clamp recording from lamina I projection neurons**
825 Neurons were visualised using a fixed stage upright microscope (SliceScope;
826 Scientifica, Uckfield, UK) equipped with a 40x water immersion objective and a CMOS
827 Camera (Prime BSI Express, Teledyne Vision Solutions, Ontario, Canada). A narrow-
828 beam infrared LED (Opto SFH 4550; Osram, Munich, Germany, emission peak, 860 nm)
829 was positioned outside the solution meniscus. Fluorescent cells and axons were visualised
830 using LED illumination (pE-300 ultra, CoolLED, Andover, UK). Whole-cell patch clamp
831 recordings were made with a pipette constructed from thin-walled single-filamented
832 borosilicate glass using a microelectrode puller (P-1000, Sutter Instrument, CA, USA).
833 Pipette resistances ranged from 6 to 10 MΩ. Electrodes were filled with an intracellular
834 solution (in mM; 130.0 K gluconate, 10.0 KCl, 2.0 $MgCl_2$, 10.0 HEPES, 0.5 EGTA, 2.0
835 ATP-Na, 0.5 GTP-Na, and 0.2% Neurobiotin, pH adjusted to 7.3 with 1.0 M KOH). Data
836 were recorded and acquired with an amplifier (Axopatch 200B; Molecular Devices,
837 Wokingham, UK). The data were low-pass filtered at 2 kHz and digitised at 10 kHz with an
838 A/D converter (Digidata 1550B; Molecular Devices, Wokingham, UK) and stored using a
839 data acquisition program (Clampex 11; Molecular Devices, Wokingham, UK).
840
841 **Optogenetic activation**
842 Two $Trpm8^{Flp}$;RCE:FRT mice were given intraperitoneal injections of
843 AAV.PHP.S.Flp^{ON}.ChR2_YFP (1.3×10^{11} GC in 10 µl) on postnatal day 2 and 5 weeks later
844 they received brain injections of AAV11.tdTomato, as described above. A blue light pulse
845 (pE-300 ultra, CoolLED, Andover, UK) was applied through the objective (40x) of the
846 microscope for 1 ms. The shutter was controlled by a TTL pulse from the A/D converter
847 (Digidata 1550B; Molecular Devices, Wokingham, UK). To determine whether the
848 recorded neuron received monosynaptic or polysynaptic input from Trpm8 afferents, we
849 applied 0.2 Hz photostimulation (1 ms pulse width) based on a previous study[44] with minor
850 modifications. Input was considered monosynaptic if there was no failure and the latency
851 jitter was smaller than 1ms.
852
853 **Natural stimulation to the skin**

854 To test whether cells with dense Trpm8 input were cold-selective, we made patch-clamp
855 recordings in mice in which Trpm8 axons were revealed with GFP and projection neurons
856 were labelled with either mCherry or tdTomato using semi-intact somatosensory
857 preparation (Fig 4A). Successful recordings were made in 6 out of 16 experiments: 5
858 Trpm8^{Flp};RCE:FRT mice (2 male, 3 female) that had received injections of AAV9.mCherry
859 into the LPB or CVLM, and one male Trpm8^{Flp};RCE:FRT;Ai9 mouse injected in the CVLM
860 with AAV9.EGFP_Cre. To test whether cells with dense Trpm8 input were cold-selective,
861 we made patch-clamp recordings in 4 Trpm8^{Flp};RCE:FRT mice (1 male, 3 female) that had
862 received injections of AAV9.mCherry into the LPB or CVLM, and one male
863 Trpm8^{Flp};RCE:FRT;Ai9 mouse injected in the CVLM with AAV9.EGFP_Cre. For the
864 investigation of Calb1-Cre-positive lamina I neurons, recordings were made in 4 female
865 Calb1^{Cre} mice that had received injections of AAV11.Cre^{ON}.tdTomato into the CVLM.
866 Recordings were initially made in voltage clamp mode (VH = -70mV) to reveal
867 spontaneous EPSCs. To find the receptive field of the recorded neurons, mechanical, hot,
868 and cold stimuli were gently applied to the skin. Mechanical stimulation was applied using
869 von Frey filaments (4-g or 10-g), and in some cases the skin was brushed with a
870 paintbrush. Hot and cold stimulation were administered by applying a small amount of
871 15˚C saline or 50˚C saline to the skin using an eye dropper. The temperature at the skin
872 surface was 20˚C and 38˚C, respectively. Once the receptive field was identified, each
873 stimulus was reapplied directly to the receptive field for 1 second. The evoked EPSCs
874 were recorded in voltage clamp mode (VH = -70mV), and the evoked action potentials
875 were recorded in current clamp mode (IH = 0 pA) or both. The events were detected with
876 Easy Electrophysiology software (Easy Electrophysiology, London, UK).
877
878 **Quantification and statistical analysis**
879 Data are reported as mean ± SD, unless stated otherwise. Statistical analyses were
880 performed using Prism software (v10, GraphPad Software, CA, USA) or SciPy library
881 (https://docs.scipy.org/doc/) in Python. The statistical tests used for each experiment,
882 including tests for multiple comparisons, are given in the appropriate figure legends. A p
883 value of <0.05 was considered significant, and significance markers are denoted within
884 figures as follows: *p < 0.05, **p < 0.01, ***p < 0.001.
885

886 **Data and materials availability**

887 Upon acceptance of this manuscript, all data will be made accessible from the Enlighten:
888 Research Data open repository hosted at the University of Glasgow. This study did not
889 generate any new materials, reagents or code.

890

891

892 **ACKNOWLEDGMENTS**

893 This research was funded in whole, or in part, by the Wellcome Trust (Grant numbers
894 219433/Z/19/Z and 304005/Z/23/Z) and the Medical Research Council (Grant number
895 MR/V033638/1). For the purpose of Open Access, the authors have applied a CC BY
896 public copyright licence to any Author Accepted Manuscript version arising from this
897 submission. We are grateful to Robert Kerr, Iain Plenderleith and Erin Dunn for expert
898 technical assistance, and to Mark Hoon and Artur Kania for the gifts of Trpm8^{Flp} and
899 Phox2a::Cre mice.

900

901 **AUTHOR CONTRIBUTIONS**

902 A.N.R., W.M., A.C.D., E.P, A.M.B., A.J.T and J.H. conceived the project and designed
903 experiments. A.J.T., A.M.B. and J.H. obtained funding. A.N.R., W.M., A.C.D., E.P., A.M.,
904 M.Y., A.H.C., D.S., A.M.B. and J.H. performed experiments. A.N.R., W.M., A.M., A.J.T.
905 and J.H. analysed data. M.W. provided reagents. A.N.R., W.M., A.M.B., A.J.T. and J.H.
906 wrote the paper. All of the authors provided feedback and contributed to editing of the
907 manuscript.

908

909 **COMPETING INTERESTS**

910 The authors declare no competing interests.

911

912 **REFERENCES**

913 1. Javed, S., Viswanathan, A., and Abdi, S. (2020). Cordotomy for intractable cancer pain: a narrative
914 review. Pain Physician *23*, 283-292.
915 2. Lahuerta, J., Bowsher, D., Campbell, J., and Lipton, S. (1990). Clinical and instrumental evaluation of
916 sensory function before and after percutaneous anterolateral cordotomy at cervical level in man.
917 Pain *42*, 23-30. 10.1016/0304-3959(90)91087-Y.
918 3. Chen, H., Bleimeister, I.H., Nguyen, E.K., Li, J., Cui, A.Y., Stratton, H.J., Smith, K.M., Baccei, M.L., and
919 Ross, S.E. (2024). The functional and anatomical characterization of three spinal output pathways of
920 the anterolateral tract. Cell reports *43*, 113829. 10.1016/j.celrep.2024.113829.
921 4. Ma, W., Dickie, A.C., Polgar, E., Yadav, M., Quillet, R., Gutierrez-Mecinas, M., Bell, A.M., and Todd,
922 A.J. (2025). Expression of Tacr1 and Gpr83 by spinal projection neurons. Molecular pain *21*,
923 17448069251342409. 10.1177/17448069251342409.
924 5. Ma, W., Polgar, E., Dickie, A.C., Hajer, M.A., Quillet, R., Gutierrez-Mecinas, M., Yadav, M.,
925 Hachisuka, J., Todd, A.J., and Bell, A.M. (2025). Anatomical characterisation of somatostatin-
926 expressing neurons belonging to the anterolateral system. Scientific reports *15*, 9549.
927 10.1038/s41598-025-93816-6.
928 6. McMahon, S.B., and Wall, P.D. (1983). A system of rat spinal cord lamina 1 cells projecting through
929 the contralateral dorsolateral funiculus. The Journal of comparative neurology *214*, 217-223.
930 10.1002/cne.902140209.
931 7. Chung, K., Kevetter, G.A., Willis, W.D., and Coggeshall, R.E. (1984). An estimate of the ratio of
932 propriospinal to long tract neurons in the sacral spinal cord of the rat. Neuroscience letters *44*, 173-
933 177. 10.1016/0304-3940(84)90077-6.
934 8. Abraira, V.E., and Ginty, D.D. (2013). The sensory neurons of touch. Neuron *79*, 618-639.
935 10.1016/j.neuron.2013.07.051.
936 9. Ma, Q. (2022). A functional subdivision within the somatosensory system and its implications for
937 pain research. Neuron *110*, 749-769. 10.1016/j.neuron.2021.12.015.
938 10. Todd, A.J. (2010). Neuronal circuitry for pain processing in the dorsal horn. Nature reviews.
939 Neuroscience *11*, 823-836. nrn2947 [pii] 10.1038/nrn2947.
940 11. Wang, L.H., Ding, W.Q., and Sun, Y.G. (2022). Spinal ascending pathways for somatosensory
941 information processing. Trends Neurosci *45*, 594-607. 10.1016/j.tins.2022.05.005.
942 12. Wercberger, R., and Basbaum, A.I. (2019). Spinal cord projection neurons: a superficial, and also
943 deep, analysis. Curr Opin Physiol *11*, 109-115. 10.1016/j.cophys.2019.10.002.
944 13. Bell, A.M., Utting, C., Dickie, A.C., Kucharczyk, M.W., Quillet, R., Gutierrez-Mecinas, M., Razlan,
945 A.N.B., Cooper, A.H., Lan, Y., Hachisuka, J., et al. (2024). Deep sequencing of Phox2a nuclei reveals
946 five classes of anterolateral system neurons. Proceedings of the National Academy of Sciences of
947 the United States of America *121*, e2314213121. 10.1073/pnas.2314213121.
948 14. Roome, R.B., Bourojeni, F.B., Mona, B., Rastegar-Pouyani, S., Blain, R., Dumouchel, A., Salesse, C.,
949 Thompson, W.S., Brookbank, M., Gitton, Y., et al. (2020). Phox2a defines a developmental origin of
950 the anterolateral system in mice and humans. Cell reports *33*, 108425.
951 10.1016/j.celrep.2020.108425.
952 15. Peier, A.M., Moqrich, A., Hergarden, A.C., Reeve, A.J., Andersson, D.A., Story, G.M., Earley, T.J.,
953 Dragoni, I., McIntyre, P., Bevan, S., and Patapoutian, A. (2002). A TRP channel that senses cold
954 stimuli and menthol. Cell *108*, 705-715. 10.1016/s0092-8674(02)00652-9.
955 16. McKemy, D.D., Neuhausser, W.M., and Julius, D. (2002). Identification of a cold receptor reveals a
956 general role for TRP channels in thermosensation. Nature *416*, 52-58. 10.1038/nature719.
957 17. Lewis, C.M., and Griffith, T.N. (2022). The mechanisms of cold encoding. Current opinion in
958 neurobiology *75*, 102571. 10.1016/j.conb.2022.102571.
959 18. Knowlton, W.M., Palkar, R., Lippoldt, E.K., McCoy, D.D., Baluch, F., Chen, J., and McKemy, D.D.
960 (2013). A sensory-labeled line for cold: TRPM8-expressing sensory neurons define the cellular basis

961 for cold, cold pain, and cooling-mediated analgesia. The Journal of neuroscience : the official
962 journal of the Society for Neuroscience *33*, 2837-2848. 10.1523/JNEUROSCI.1943-12.2013.
963 19. Pogorzala, L.A., Mishra, S.K., and Hoon, M.A. (2013). The cellular code for mammalian
964 thermosensation. The Journal of neuroscience : the official journal of the Society for Neuroscience
965 *33*, 5533-5541. 10.1523/JNEUROSCI.5788-12.2013.
966 20. Takashima, Y., Daniels, R.L., Knowlton, W., Teng, J., Liman, E.R., and McKemy, D.D. (2007). Diversity
967 in the neural circuitry of cold sensing revealed by genetic axonal labeling of transient receptor
968 potential melastatin 8 neurons. The Journal of neuroscience : the official journal of the Society for
969 Neuroscience *27*, 14147-14157. 10.1523/JNEUROSCI.4578-07.2007.
970 21. Kim, Y.S., Park, J.H., Choi, S.J., Bae, J.Y., Ahn, D.K., McKemy, D.D., and Bae, Y.C. (2014). Central
971 connectivity of transient receptor potential melastatin 8-expressing axons in the brain stem and
972 spinal dorsal horn. PloS one *9*, e94080. 10.1371/journal.pone.0094080.
973 22. Dhaka, A., Earley, T.J., Watson, J., and Patapoutian, A. (2008). Visualizing cold spots: TRPM8-
974 expressing sensory neurons and their projections. The Journal of neuroscience : the official journal
975 of the Society for Neuroscience *28*, 566-575. 28/3/566 [pii] 10.1523/JNEUROSCI.3976-07.2008.
976 23. Craig, A.D., and Kniffki, K.D. (1985). Spinothalamic lumbosacral lamina I cells responsive to skin and
977 muscle stimulation in the cat. The Journal of physiology *365*, 197-221.
978 10.1113/jphysiol.1985.sp015767.
979 24. Craig, A.D., Krout, K., and Andrew, D. (2001). Quantitative response characteristics of
980 thermoreceptive and nociceptive lamina I spinothalamic neurons in the cat. Journal of
981 neurophysiology *86*, 1459-1480. 10.1152/jn.2001.86.3.1459.
982 25. Craig, A.D., and Dostrovsky, J.O. (2001). Differential projections of thermoreceptive and nociceptive
983 lamina I trigeminothalamic and spinothalamic neurons in the cat. Journal of neurophysiology *86*,
984 856-870. 10.1152/jn.2001.86.2.856.
985 26. Craig, A.D., and Hunsley, S.J. (1991). Morphine enhances the activity of thermoreceptive cold-
986 specific lamina I spinothalamic neurons in the cat. Brain research *558*, 93-97. 10.1016/0006-
987 8993(91)90719-c.
988 27. Dostrovsky, J.O., and Craig, A.D. (1996). Cooling-specific spinothalamic neurons in the monkey.
989 Journal of neurophysiology *76*, 3656-3665. 10.1152/jn.1996.76.6.3656.
990 28. Zhang, X., Davidson, S., and Giesler, G.J., Jr. (2006). Thermally identified subgroups of marginal zone
991 neurons project to distinct regions of the ventral posterior lateral nucleus in rats. The Journal of
992 neuroscience : the official journal of the Society for Neuroscience *26*, 5215-5223.
993 10.1523/JNEUROSCI.0701-06.2006.
994 29. Allard, J. (2019). Physiological properties of the lamina I spinoparabrachial neurons in the mouse.
995 The Journal of physiology *597*, 2097-2113. 10.1113/JP277447.
996 30. Andrew, D. (2009). Sensitization of lamina I spinoparabrachial neurons parallels heat hyperalgesia
997 in the chronic constriction injury model of neuropathic pain. The Journal of physiology *587*, 2005-
998 2017.
999 31. Hachisuka, J., Baumbauer, K.M., Omori, Y., Snyder, L.M., Koerber, H.R., and Ross, S.E. (2016). Semi-
1000 intact ex vivo approach to investigate spinal somatosensory circuits. Elife *5*, e22866.
1001 10.7554/eLife.22866.
1002 32. Hachisuka, J., Koerber, H.R., and Ross, S.E. (2020). Selective-cold output through a distinct subset of
1003 lamina I spinoparabrachial neurons. Pain *161*, 185-194. 10.1097/j.pain.0000000000001710.
1004 33. Chisholm, K.I., Lo Re, L., Polgar, E., Gutierrez-Mecinas, M., Todd, A.J., and McMahon, S.B. (2021).
1005 The encoding of cutaneous stimuli by lamina I projection neurons. Pain *162*, 2405-2417.
1006 10.1097/j.pain.0000000000002226.
1007 34. Lee, H., Hor, C.C., Horwitz, L.R., Xiong, A., Su, X.Y., Soden, D.R., Yang, S., Cai, W., Zhang, W., Li, C., et
1008 al. (2025). A dedicated skin-to-brain circuit for cool sensation in mice. Nature communications *16*,
1009 6731. 10.1038/s41467-025-61562-y.
1010 35. Qi, L., Iskols, M., Shi, D., Reddy, P., Walker, C., Lezgiyeva, K., Voisin, T., Pawlak, M., Kuchroo, V.K.,
1011 Chiu, I.M., et al. (2024). A mouse DRG genetic toolkit reveals morphological and physiological

1012 diversity of somatosensory neuron subtypes. Cell *187*, 1508-1526 e1516.
1013 10.1016/j.cell.2024.02.006.
1014 36. Sharma, N., Flaherty, K., Lezgiyeva, K., Wagner, D.E., Klein, A.M., and Ginty, D.D. (2020). The
1015 emergence of transcriptional identity in somatosensory neurons. Nature *577*, 392-398.
1016 10.1038/s41586-019-1900-1.
1017 37. Zeisel, A., Hochgerner, H., Lonnerberg, P., Johnsson, A., Memic, F., van der Zwan, J., Haring, M.,
1018 Braun, E., Borm, L.E., La Manno, G., et al. (2018). Molecular Architecture of the Mouse Nervous
1019 System. Cell *174*, 999-1014 e1022. 10.1016/j.cell.2018.06.021.
1020 38. Li, J., Kritzer, E., Craig, P.E., and Baccei, M.L. (2015). Aberrant synaptic integration in adult lamina I
1021 projection neurons following neonatal tissue damage. The Journal of neuroscience : the official
1022 journal of the Society for Neuroscience *35*, 2438-2451. 10.1523/JNEUROSCI.3585-14.2015.
1023 39. Seal, R.P., Wang, X., Guan, Y., Raja, S.N., Woodbury, C.J., Basbaum, A.I., and Edwards, R.H. (2009).
1024 Injury-induced mechanical hypersensitivity requires C-low threshold mechanoreceptors. Nature
1025 *462*, 651-655.
1026 40. Dickie, A.C., Bell, A.M., Iwagaki, N., Polgar, E., Gutierrez-Mecinas, M., Kelly, R., Lyon, H., Turnbull, K.,
1027 West, S.J., Etlin, A., et al. (2019). Morphological and functional properties distinguish the substance
1028 P and gastrin-releasing peptide subsets of excitatory interneuron in the spinal cord dorsal horn.
1029 Pain *160*, 442-462. 10.1097/j.pain.0000000000001406.
1030 41. Ordas, P., Hernandez-Ortego, P., Vara, H., Fernandez-Pena, C., Reimundez, A., Morenilla-Palao, C.,
1031 Guadano-Ferraz, A., Gomis, A., Hoon, M., Viana, F., and Senaris, R. (2021). Expression of the cold
1032 thermoreceptor TRPM8 in rodent brain thermoregulatory circuits. The Journal of comparative
1033 neurology *529*, 234-256. 10.1002/cne.24694.
1034 42. Gutierrez-Mecinas, M., Kuehn, E.D., Abraira, V.E., Polgár, E., Watanabe, M., and Todd, A.J. (2016).
1035 Immunostaining for Homer reveals the majority of excitatory synapses in laminae I-III of the mouse
1036 spinal dorsal horn. Neuroscience *329*, 171-181. 10.1016/j.neuroscience.2016.05.009.
1037 43. Todd, A.J. (1997). A method for combining confocal and electron microscopic examination of
1038 sections processed for double- or triple-labelling immunocytochemistry. Journal of neuroscience
1039 methods *73*, 149-157. S0165-0270(97)02222-X [pii].
1040 44. Hachisuka, J., Omori, Y., Chiang, M.C., Gold, M.S., Koerber, H.R., and Ross, S.E. (2018). Wind-up in
1041 lamina I spinoparabrachial neurons: a role for reverberatory circuits. Pain *159*, 1484-1493.
1042 10.1097/j.pain.0000000000001229.
1043 45. Menetrey, D., De Pommery, J., Thomasset, M., and Baimbridge, K.G. (1992). Calbindin-D28K
1044 (CaBP28k)-like Immunoreactivity in Ascending Projections. The European journal of neuroscience *4*,
1045 70-76. 10.1111/j.1460-9568.1992.tb00110.x.
1046 46. Alsulaiman, W.A.A., Quillet, R., Bell, A.M., Dickie, A.C., Polgar, E., Boyle, K.A., Watanabe, M.,
1047 Roome, R.B., Kania, A., Todd, A.J., and Gutierrez-Mecinas, M. (2021). Characterisation of lamina I
1048 anterolateral system neurons that express Cre in a Phox2a-Cre mouse line. Scientific reports *11*,
1049 17912. 10.1038/s41598-021-97105-w.
1050 47. Han, Z., Luo, N., Ma, W., Liu, X., Cai, Y., Kou, J., Wang, J., Li, L., Peng, S., Xu, Z., et al. (2023). AAV11
1051 enables efficient retrograde targeting of projection neurons and enhances astrocyte-directed
1052 transduction. Nature communications *14*, 3792. 10.1038/s41467-023-39554-7.
1053 48. Cano, G., Passerin, A.M., Schiltz, J.C., Card, J.P., Morrison, S.F., and Sved, A.F. (2003). Anatomical
1054 substrates for the central control of sympathetic outflow to interscapular adipose tissue during cold
1055 exposure. The Journal of comparative neurology *460*, 303-326. 10.1002/cne.10643.
1056 49. Geerling, J.C., Kim, M., Mahoney, C.E., Abbott, S.B., Agostinelli, L.J., Garfield, A.S., Krashes, M.J.,
1057 Lowell, B.B., and Scammell, T.E. (2016). Genetic identity of thermosensory relay neurons in the
1058 lateral parabrachial nucleus. Am J Physiol Regul Integr Comp Physiol *310*, R41-54.
1059 10.1152/ajpregu.00094.2015.
1060 50. Yang, W.Z., Xie, H., Du, X., Zhou, Q., Xiao, Y., Zhao, Z., Jia, X., Xu, J., Zhang, W., Cai, S., et al. (2023). A
1061 parabrachial-hypothalamic parallel circuit governs cold defense in mice. Nature communications
1062 *14*, 4924. 10.1038/s41467-023-40504-6.

1063 51. Yoshida, K., Konishi, M., Nagashima, K., Saper, C.B., and Kanosue, K. (2005). Fos activation in
1064 hypothalamic neurons during cold or warm exposure: projections to periaqueductal gray matter.
1065 Neuroscience *133*, 1039-1046. 10.1016/j.neuroscience.2005.03.044.
1066 52. Vestergaard, M., Carta, M., Guney, G., and Poulet, J.F.A. (2023). The cellular coding of temperature
1067 in the mammalian cortex. Nature *614*, 725-731. 10.1038/s41586-023-05705-5.
1068 53. Leva, T.M., and Whitmire, C.J. (2023). Thermosensory thalamus: parallel processing across model
1069 organisms. Front Neurosci *17*, 1210949. 10.3389/fnins.2023.1210949.
1070 54. Bernard, J.F., Dallel, R., Raboisson, P., Villanueva, L., and Le Bars, D. (1995). Organization of the
1071 efferent projections from the spinal cervical enlargement to the parabrachial area and
1072 periaqueductal gray: a PHA-L study in the rat. The Journal of comparative neurology *353*, 480-505.
1073 10.1002/cne.903530403.
1074 55. Feil, K., and Herbert, H. (1995). Topographic organization of spinal and trigeminal somatosensory
1075 pathways to the rat parabrachial and Kolliker-Fuse nuclei. The Journal of comparative neurology
1076 *353*, 506-528. 10.1002/cne.903530404.
1077 56. Gauriau, C., and Bernard, J.F. (2004). A comparative reappraisal of projections from the superficial
1078 laminae of the dorsal horn in the rat: the forebrain. The Journal of comparative neurology *468*, 24-
1079 56. 10.1002/cne.10873.
1080 57. Gutierrez-Mecinas, M., Polgar, E., Bell, A.M., Herau, M., and Todd, A.J. (2018). Substance P-
1081 expressing excitatory interneurons in the mouse superficial dorsal horn provide a propriospinal
1082 input to the lateral spinal nucleus. Brain structure & function *223*, 2377-2392. 10.1007/s00429-018-
1083 1629-x.
1084 58. Gutierrez-Mecinas, M., Bell, A., Polgar, E., Watanabe, M., and Todd, A.J. (2019). Expression of
1085 neuropeptide FF defines a population of excitatory interneurons in the superficial dorsal horn of
1086 the mouse spinal cord that respond to noxious and pruritic stimuli. Neuroscience *416*, 281-293.
1087 10.1016/j.neuroscience.2019.08.013.
1088 59. Polgár, E., Dickie, A.C., Gutierrez-Mecinas, M., Bell, A.M., Boyle, K.A., Quillet, R., Ab Rashid, E., Clark,
1089 R.A., German, M.T., Watanabe, M., et al. (2023). Grpr expression defines a population of superficial
1090 dorsal horn vertical cells that have a role in both itch and pain. Pain *164*, 149-170.
1091 10.1097/j.pain.0000000000002677.
1092 60. Choi, S., Hachisuka, J., Brett, M.A., Magee, A.R., Omori, Y., Iqbal, N.U., Zhang, D., DeLisle, M.M.,
1093 Wolfson, R.L., Bai, L., et al. (2020). Parallel ascending spinal pathways for affective touch and pain.
1094 Nature *587*, 258-263. 10.1038/s41586-020-2860-1.
1095 61. Al-Khater, K.M., Kerr, R., and Todd, A.J. (2008). A quantitative study of spinothalamic neurons in
1096 laminae I, III, and IV in lumbar and cervical segments of the rat spinal cord. The Journal of
1097 comparative neurology *511*, 1-18.
1098 62. Franklin, K.B.J., and Paxinos, G. (2007). The Mouse Brain in Stereotaxic Coordinates. Third Edition
1099 (Elsevier).
1100 63. Al-Khater, K.M., and Todd, A.J. (2009). Collateral projections of neurons in laminae I, III, and IV of
1101 rat spinal cord to thalamus, periaqueductal gray matter, and lateral parabrachial area. The Journal
1102 of comparative neurology *515*, 629-646.
1103 64. Ma, W., Dickie, A., Polgar, E., Yadav, M., Quillet, R., Gutierrez-Mecinas, M., Bell, A.M., and Todd, A.
1104 (2025). Expression of Tacr1 and Gpr83 by spinal projection neurons. Molecular pain,
1105 17448069251342409. 10.1177/17448069251342409.
1106 65. Ding, Y.Q., Takada, M., Shigemoto, R., and Mizumo, N. (1995). Spinoparabrachial tract neurons
1107 showing substance P receptor-like immunoreactivity in the lumbar spinal cord of the rat. Brain
1108 research *674*, 336-340. 000689939500022I [pii].
1109 66. Marshall, G.E., Shehab, S.A., Spike, R.C., and Todd, A.J. (1996). Neurokinin-1 receptors on lumbar
1110 spinothalamic neurons in the rat. Neuroscience *72*, 255-263. 0306452295005587 [pii].
1111 67. McKemy, D.D. (2013). The molecular and cellular basis of cold sensation. ACS Chem Neurosci *4*,
1112 238-247. 10.1021/cn300193h.

1113 68. Ren, X., Liu, S., Virlogeux, A., Kang, S.J., Brusch, J., Liu, Y., Dymecki, S.M., Han, S., Goulding, M., and
1114 Acton, D. (2023). Identification of an essential spinoparabrachial pathway for mechanical itch.
1115 Neuron *111*, 1812-1829 e1816. 10.1016/j.neuron.2023.03.013.
1116 69. Madisen, L., Zwingman, T.A., Sunkin, S.M., Oh, S.W., Zariwala, H.A., Gu, H., Ng, L.L., Palmiter, R.D.,
1117 Hawrylycz, M.J., Jones, A.R., et al. (2010). A robust and high-throughput Cre reporting and
1118 characterization system for the whole mouse brain. Nature neuroscience *13*, 133-140. nn.2467 [pii]
1119 10.1038/nn.2467.
1120 70. Morrison, S.F. (2018). Efferent neural pathways for the control of brown adipose tissue
1121 thermogenesis and shivering. Handb Clin Neurol *156*, 281-303. 10.1016/B978-0-444-63912-
1122 7.00017-5.
1123 71. Li, J., Serafin, E.K., and Baccei, M.L. (2023). Intrinsic and synaptic properties of adult mouse
1124 spinoperiaqueductal gray neurons and the influence of neonatal tissue damage. Pain *164*, 905-917.
1125 10.1097/j.pain.0000000000002787.
1126 72. Spike, R.C., Puskar, Z., Andrew, D., and Todd, A.J. (2003). A quantitative and morphological study of
1127 projection neurons in lamina I of the rat lumbar spinal cord. The European journal of neuroscience
1128 *18*, 2433-2448.
1129 73. Chen, X.M., Nishi, M., Taniguchi, A., Nagashima, K., Shibata, M., and Kanosue, K. (2002). The caudal
1130 periaqueductal gray participates in the activation of brown adipose tissue in rats. Neuroscience
1131 letters *331*, 17-20. 10.1016/s0304-3940(02)00757-7.
1132 74. Sousa, V.H., Miyoshi, G., Hjerling-Leffler, J., Karayannis, T., and Fishell, G. (2009). Characterization
1133 of Nkx6-2-derived neocortical interneuron lineages. Cerebral cortex *19 Suppl 1*, i1-10.
1134 10.1093/cercor/bhp038.
1135 75. Daigle, T.L., Madisen, L., Hage, T.A., Valley, M.T., Knoblich, U., Larsen, R.S., Takeno, M.M., Huang, L.,
1136 Gu, H., Larsen, R., et al. (2018). A suite of transgenic driver and reporter mouse lines with enhanced
1137 brain-cell-type targeting and functionality. Cell *174*, 465-480 e422. 10.1016/j.cell.2018.06.035.
1138 76. Quillet, R., Gutierrez-Mecinas, M., Polgar, E., Dickie, A.C., Boyle, K.A., Watanabe, M., and Todd, A.J.
1139 (2023). Synaptic circuits involving gastrin-releasing peptide receptor-expressing neurons in the
1140 dorsal horn of the mouse spinal cord. Front Mol Neurosci *16*, 1294994.
1141 10.3389/fnmol.2023.1294994.
1142 77. Bell, A.M., Gutierrez-Mecinas, M., Stevenson, A., Casas-Benito, A., Wildner, H., West, S.J.,
1143 Watanabe, M., and Todd, A.J. (2020). Expression of green fluorescent protein defines a specific
1144 population of lamina II excitatory interneurons in the GRP::eGFP mouse. Scientific reports *10*,
1145 13176. 10.1038/s41598-020-69711-7.
1146 78. Polgár, E., Gray, S., Riddell, J.S., and Todd, A.J. (2004). Lack of evidence for significant neuronal loss
1147 in laminae I-III of the spinal dorsal horn of the rat in the chronic constriction injury model. Pain *111*,
1148 144-150. 10.1016/j.pain.2004.06.011 S0304395904002994 [pii].

1149

1150

1151 **MAIN FIGURES**

1152 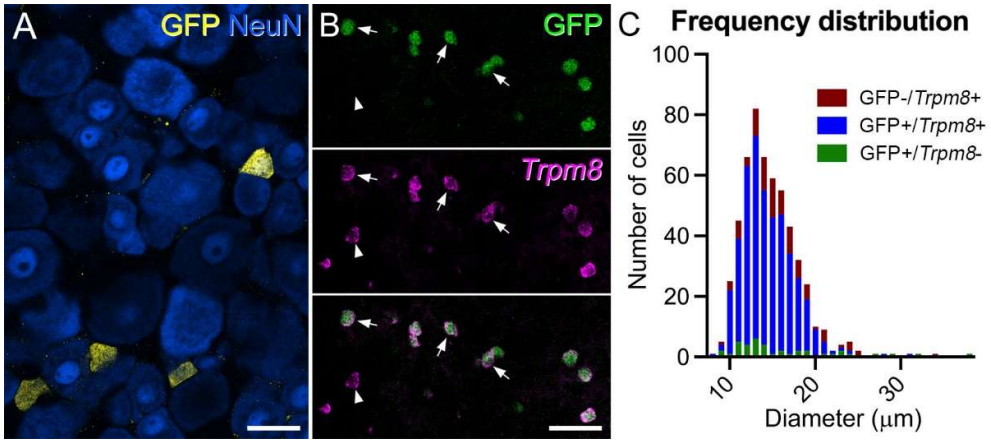

1153 **Figure 1. The Trpm8^{Flp} mouse line captures Trpm8-expressing primary afferent**
1154 **neurons.** (**A**) Immunohistochemical staining for GFP (yellow) and NeuN (blue) in a dorsal
1155 root ganglion from a Trpm8^{Flp};RCE:FRT mouse. GFP is present in some of the small
1156 neurons. (**B**) Fluorescence *in situ* hybridisation with a probe for *Trpm8* mRNA (magenta)
1157 superimposed on GFP native fluorescence (green). The great majority of GFP cells
1158 contain *Trpm8* message, and *vice versa*. Some of the double-labelled cells are indicated
1159 with arrows, while the arrowhead points to a *Trpm8*-positive cell that lacks GFP. (**C**)
1160 Frequency distribution of soma diameter for cells that were GFP-/*Trpm8*+ (red bars),
1161 GFP+/*Trpm8*+ (blue bars) or GFP+/*Trpm8*- (green bars). Scale bars: (**A**) = 25 µm, (**B**) = 50
1162 µm.

1163

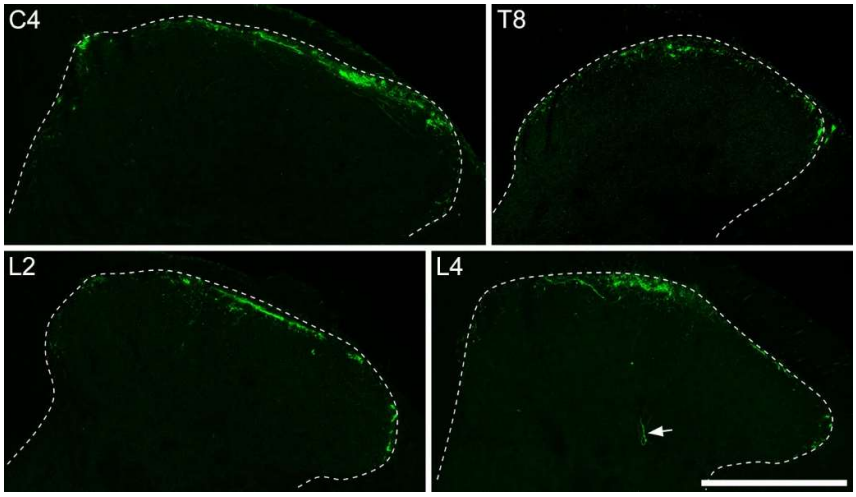

Figure 2. Distribution of Trpm8 afferents in the spinal dorsal horn.
Immunohistochemical staining for GFP at different segmental levels through the spinal cord in Trpm8^{Flp};RCE:FRT mice. GFP-labelled axons are largely restricted to lamina I, although occasional fibres penetrate into deeper parts of the dorsal horn (arrow). Within lamina I the distribution of GFP axons is patchy, and does not occupy the entire mediolateral extent. Scale bar = 200 μm.

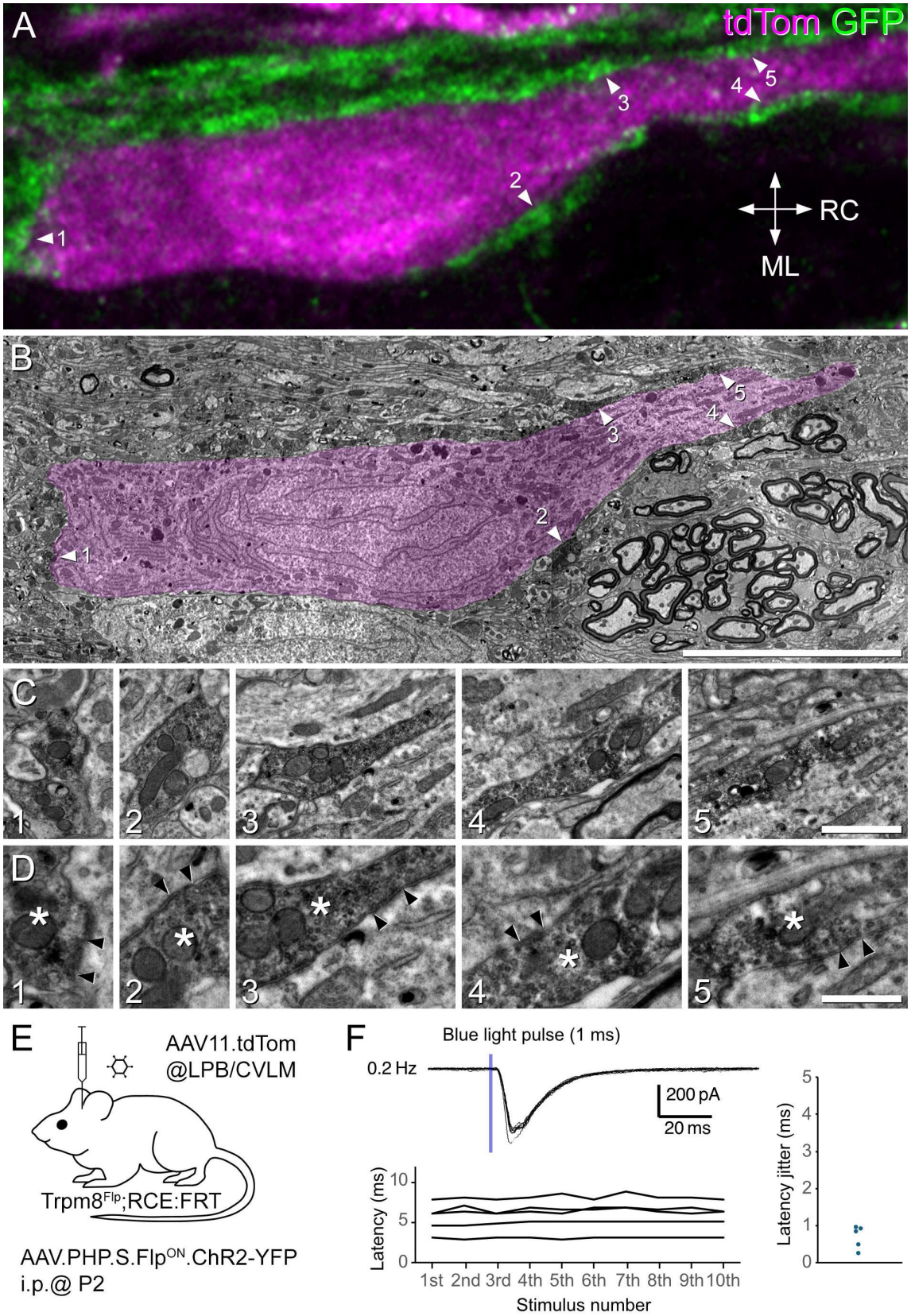

1173

Click here to enter text.

1174 **Figure 3. Evidence for monosynaptic input from Trpm8 afferents to lamina I ALS**
1175 **neurons that were surrounded by these afferents.** (**A**-**D**) Combined confocal and
1176 electron microscopic examination of a lamina I projection neuron with numerous contacts
1177 from Trpm8-expressing afferents. (**A**) A confocal image (single optical section) from a
1178 horizontal section through lamina I, showing the cell body and part of a proximal dendrite
1179 of one of the tdTomato-expressing neurons that were analysed. The tissue was obtained
1180 from a Phox2a::Cre;Ai9;Trpm8^{Flp};RCE:FRT mouse. TdTomato expressed by the projection
1181 neuron is shown in magenta and GFP immunoreactivity in Trpm8 afferents in green.
1182 Several Trpm8 boutons contact the cell, and five of these are indicated with arrowheads.
1183 RC, rostro-caudal; ML, mediolateral. (**B**) A low magnification electron micrograph through
1184 the cell at approximately the same z-level as that shown in **A**. Although the cell does not
1185 contain an electron dense label, it can be recognised by its shape, and because it is
1186 surrounded by GFP-expressing axonal profiles that were labelled with an
1187 immunoperoxidase method. The locations of those corresponding to the boutons shown in
1188 **A** are again marked with arrowheads. The cell has been pseudocoloured magenta to show
1189 its location. (**C**,**D**) Progressively higher magnification EM images showing the five GFP-
1190 labelled boutons marked with arrowheads in **A** and **B**. In **D** the boutons are marked with
1191 asterisks and the locations of membrane darkening and vesicle clusters that presumably
1192 correspond to synapses on the cell body and dendrite of the projection neuron are
1193 indicated with arrowheads. (**E**) The experimental approach used for optogenetic testing of
1194 Trpm8 input to ALS neurons. Stimulation (1 ms, 0.2 Hz) evoked EPSCs in 5 of the ALS
1195 neurons that were densely coated by Trpm8 afferents. (**F**) shows an example of the
1196 response in one cell (upper trace), the latencies of EPSCs in in response to 10
1197 consecutive stimuli (n = 5, lower graph), and on the right, the latency jitter for each of
1198 these cells (n = 5). Scale bars: (**A**,**B**) = 10 μm, (**C**) = 1 μm (**D**) = 500 nm.
1199

Click here to enter text.

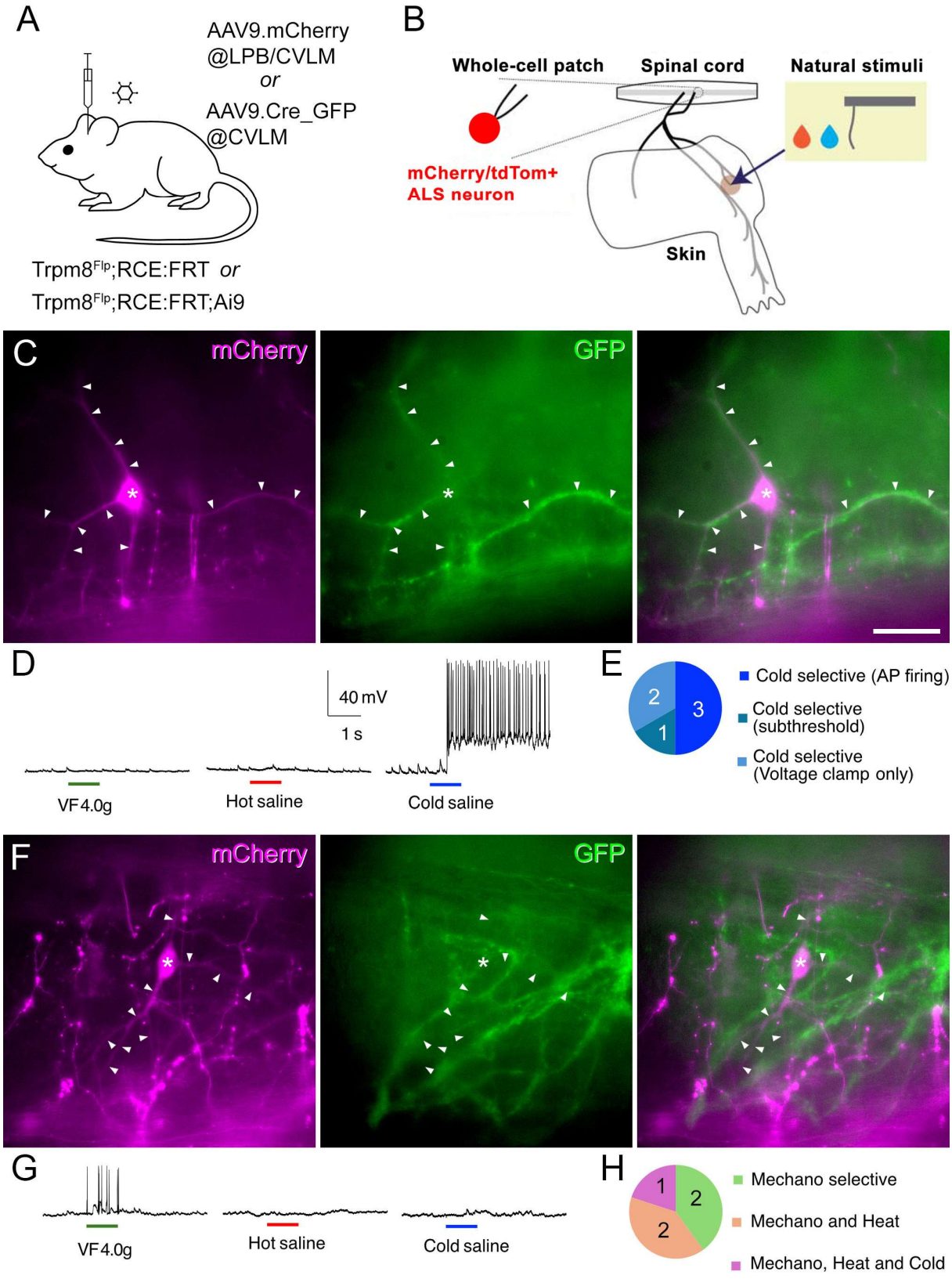

Figure 4. Electrophysiological characterisation of retrogradely labelled lamina I projection neurons recorded in Trpm8^{Flp};RCE:FRT mice (**A**) Cells were identified by

Click here to enter text.

1203 expression of mCherry following injection of AAV9.mCherry into the CVLM or LPB of
1204 Trpm8^{Flp};RCE:FRT mice, or by expression of tdTomato following injection of
1205 AAV9.Cre_GFP into the CVLM of Trpm8^{Flp};RCE:FRT;Ai9 mice. Note that the level of GFP
1206 expression resulting from injection of AAV9.Cre_GFP was extremely low, and would have
1207 been restricted to the nucleus of labelled neurons, due to the presence of a nuclear
1208 localisation signal. In both cases, Trpm8-expressing afferents were labelled with GFP. (**B**)
1209 The semi-intact somatosensory preparation retained skin attached to lumbar spinal cord
1210 through intact peripheral nerves and was used for recording responses to natural skin
1211 stimuli: Hot saline (50°C), Cold saline (15°C) or von Frey filaments (4 or 10 g) (**C**)
1212 Fluorescence microscopy image of a retrogradely labelled (mCherry-positive) lamina I ALS
1213 neuron (soma marked with asterisk) that is densely coated by Trpm8-expressing (GFP-
1214 positive) axons. Note that bundles of GFP axons are closely associated with the dendrites
1215 of the retrogradely labelled neuron, which are marked with arrowheads. (**D**) Whole-cell
1216 recording from this cell reveals that only cold stimulation evoked action potentials (APs).
1217 (**E**) Pie chart showing the response properties of the 6 lamina I ALS neurons that were
1218 densely coated with Trpm8 afferents to mechanical, cold and heat stimulation of the skin.
1219 All of these cells responded only to cold stimulation: 3 cells showed APs, 1 cell showed
1220 EPSPs but no APs (subthreshold), while 2 cells were recorded in voltage clamp and
1221 showed EPSCs. (**F**) Fluorescence microscopy image of a lamina I ALS neuron that was
1222 not densely coated with Trpm8 axons. Again, the soma is marked with an asterisk and
1223 dendrites with arrowheads. Note that although the dendrites of this cell pass through
1224 bundles of GFP axons these bundles are not aligned with the dendrites. (**G**) Whole-cell
1225 recording from the cell shown in (**F**). AP firing was evoked by mechanical stimulation (von
1226 Frey filament 4.0g), but not by application of hot or cold saline to the skin. (**H**) Pie chart of
1227 response properties of 5 lamina I ALS neurons that lacked dense Trpm8 input to
1228 mechanical, cold and heat stimulation to the skin. Two cells were mechano-selective, while
1229 three were polymodal (2 cells: mechano, heat, 1 cell: mechano, heat and cold). Scale bar
1230 (**C**,**F**) = 50 µm. Scale bars in **D** apply to **G**.
1231

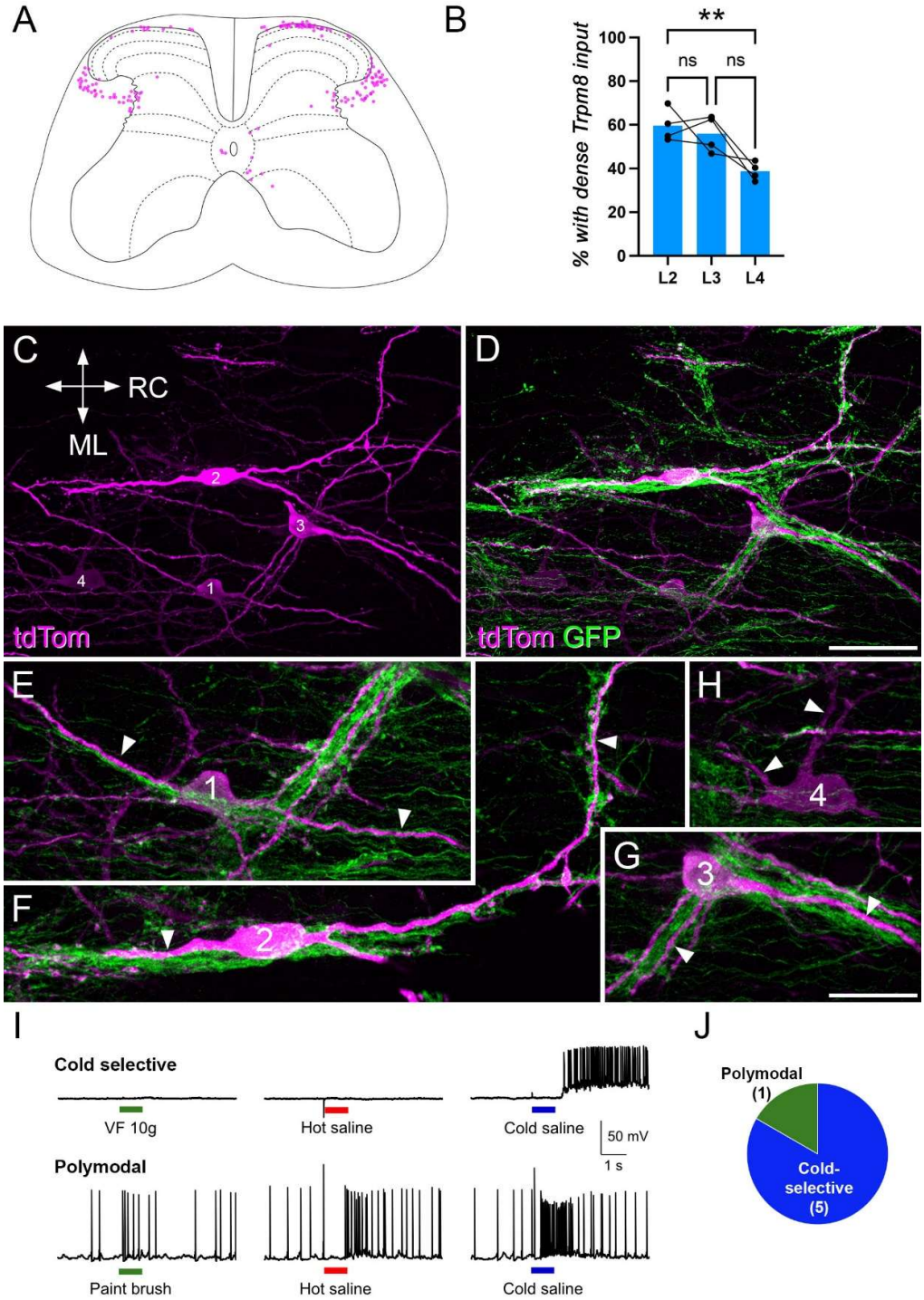

Figure 5 Characterisation of Calb1-expressing projection neurons. (**A**) The distribution of retrogradely labelled cells in 10 transverse sections from the L5 segment of one of the Calb1^{Cre} mice that had received an injection of AAV11.Cre^{ON}.tdTomato into the LPB. The right side of the plot is the side contralateral to the brain injection. (**B**) Bar chart

showing the proportion of retrogradely labelled cells in the L2, L3 and L4 segments of the Calb1^{Cre} mice injected with AAV11.Cre^{ON}.tdTomato into the LPB that received dense Trpm8 input. Repeated measures 1-way ANOVA showed a significant difference ($p = 0.048$), and post-hoc Holm-Šídák's multiple comparisons test revealed a difference only between L2 and L4 ($p = 0.0056$). (**C**) Part of a horizontal section through the L2 segment of one of the mice, showing 4 lamina I neurons (numbered 1-4) that were retrogradely labelled with tdTomato (tdTom, magenta). RC, rostrocaudal; ML, mediolateral (applies to **C**-**H**). (**D**) The same field scanned to reveal both tdTomato and GFP (green). (**E**-**H**) detailed views of the 4 cells shown in **C**,**D**. Three of these cells (1-3) have numerous contacts from GFP-labelled axons on their dendrites (marked with arrowheads) and cell bodies. The fourth cell (4) has very few such contacts. (**I**) Recordings from one of the cold-selective cells (upper traces) and the polymodal cell (lower traces) in experiments carried out in Calb1^{Cre} mice that had received injections of AAV11.Cre^{ON}.tdTomato into the CVLM. The cell in the upper traces shows action potential firing in response to application of cold saline to the skin, but no response to application of a 10g von Frey (VF) hair or hot saline. The other cell responds to brushing of the skin with a paint brush, as well as to application of hot and cold saline. (**J**) Pie chart showing response characteristics of the 6 cells recorded in these experiments. Scale bars: (**C**,**D**) = 50 μm, (**E**-**H**) = 25 μm. **P<0.01.

Click here to enter text.

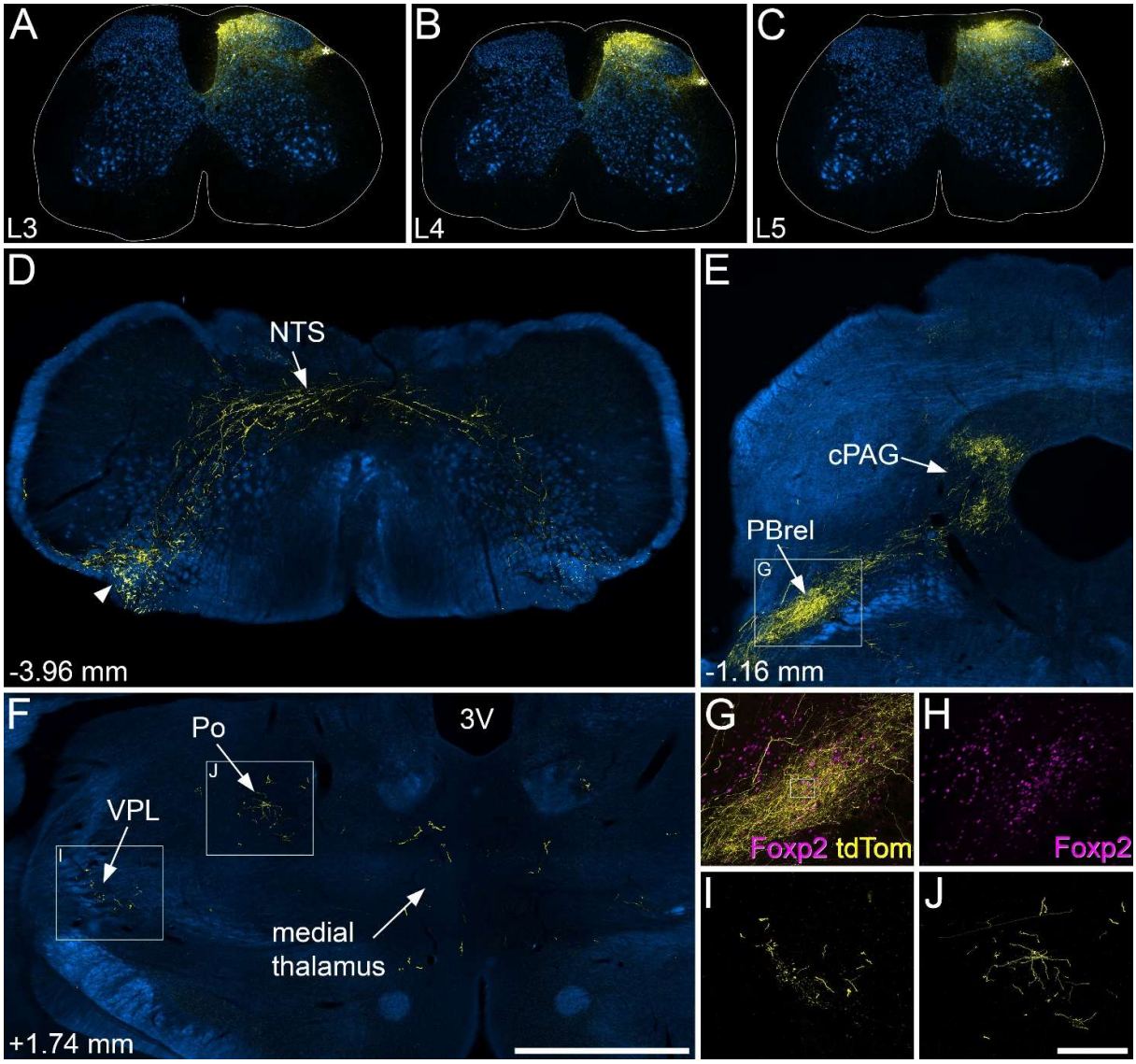

1257

1258 **Figure 6. Anterograde tracing following injections of AAV1.Cre^{ON}.tdTomato into the**
1259 **medial dorsal horn of Calb1^{Cre} mice** (**A**-**C**) Injection sites in the medial parts of the L3,
1260 L4 and L5 segments of one of the mice used in this part of the study. Immunostaining for
1261 tdTomato is shown in yellow and for NeuN in blue. Labelling of cell bodies is largely
1262 restricted to the medial part of the dorsal horn. There is some labelling in the lateral spinal
1263 nucleus (LSN), marked by asterisks, but this is likely to result from transport in axons of
1264 local interneurons. (**D**-**F**) Sections through selected regions of the brain immunostained to
1265 reveal tdTomato (yellow), with the corresponding dark-field images shown in blue. (**D**) At
1266 the level of the caudal medulla, the main ascending fibre bundle (arrowhead) lies in the
1267 ventrolateral region on the side contralateral to the spinal injections. Collateral axons
1268 innervate the nucleus of the solitary tract (NTS). (**E**) There is a dense projection of axons

1269 to the rostralmost part of the lateral parabrachial area (PBrel) and the caudal part of the
1270 PAG (cPAG) on the side contralateral to the injections. (**F**) Within the diencephalon there
1271 is sparse labelling in the contralateral ventral posterolateral nucleus (VPL) and posterior
1272 nucleus (Po) as well as within the medial thalamus. (**G**,**H**) The region indicated in the box
1273 in **E** is shown at higher magnification with immunostaining for Foxp2 shown in magenta.
1274 The overlap between arborisation of tdTomato and Foxp2-positive nuclei indicates that this
1275 region is indeed PBrel. The box in (**G**) corresponds to the region shown at higher
1276 magnification in Figure 6–figure supplement 2F. (**I**, **J**) show higher magnification views of
1277 tdTomato-positive axons in the VPL and Po, respectively, corresponding to the boxes in
1278 (**F**). Numbers in **D**-**F** show approximate rostrocaudal locations in relation to the interaural
1279 line. Images in **A**-**E**, **G**-**H** are from animal #8, and those in **F**, **I**, **J** are from animal #7 in
1280 Table 1. Scale bars: (**A**-**F**) = 1 mm, (**G**-**J**) = 200 μm.

1281

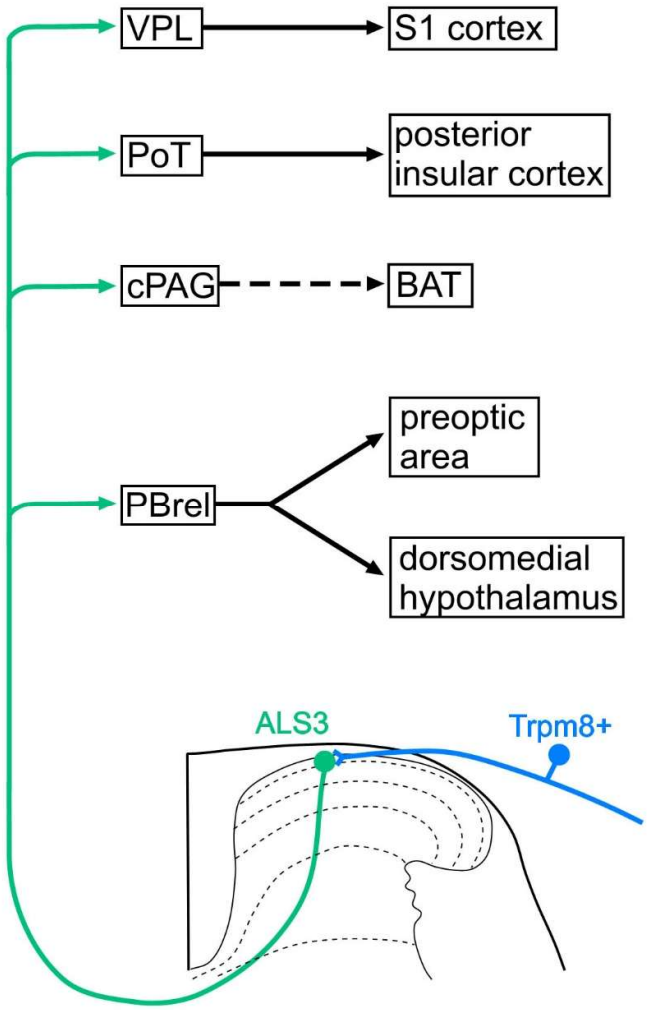

1282

1283

1284 **Figure 7. Proposed circuits involving cold-selective lamina I ALS neurons** Our results
1285 suggest that cold-selective lamina I projection neurons, which belong to the ALS3 cluster[13]
1286 project, among other sites, to PBrel, the caudal part of the PAG (cPAG) and the ventral
1287 posterolateral nucleus of the thalamus (VPL). Cold-responsive cells in PBrel innervate the
1288 preoptic area and dorsomedial hypothalamus, which are integral components of circuits
1289 that underlie cold defence. The cPAG can indirectly activate brown adipose tissue (BAT)
1290 metabolism, also contributing to cold defence. The projection to PoT and VPL, through
1291 their connections to the posterior insular and primary somatosensory (S1) cortices,
1292 presumably underlies conscious perception of cold stimuli applied to the skin. Although we
1293 show a single ALS3 neuron projecting to different brain regions, it is possible that
1294 branches to different brain nuclei originate from specific subsets of ALS3 neurons. Note

1295 that in addition to the direct (monosynaptic) input from Trpm8-expressing primary afferents
1296 to ALS3 neurons, there may also be indirect (e.g. polysynaptic) inputs arriving via
1297 excitatory interneurons.

1298

1299 **FIGURE SUPPLEMENTS**

1300

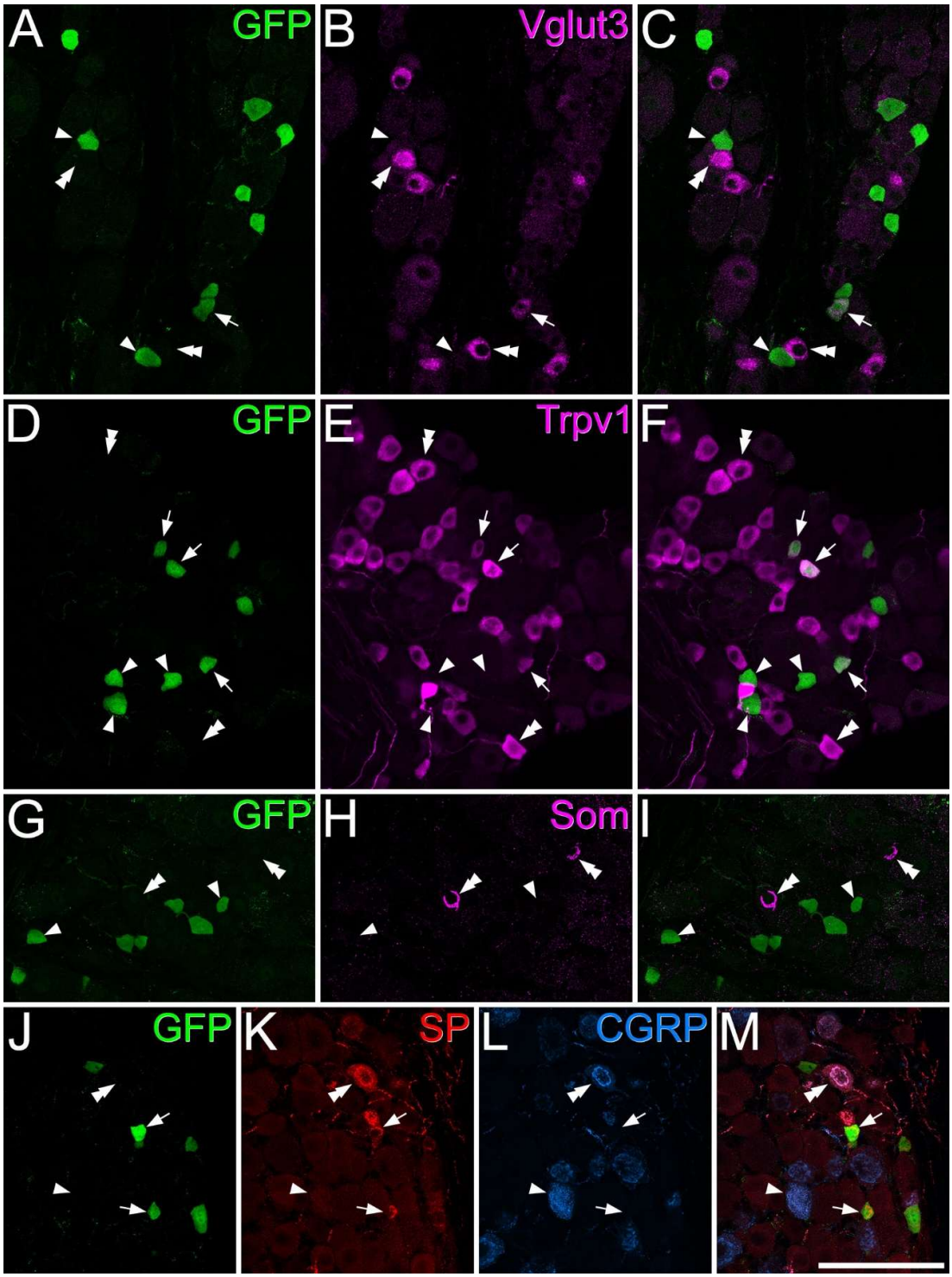

1301

1302 **Figure 1–figure supplement 1. Immunohistochemical characterisation of GFP-**
1303 **expressing somata in dorsal root ganglia of Trpm8^{Flp};RCE:FRT mice.** In each set of
1304 images GFP immunoreactivity is shown in green and other types of immunoreactivity in

1305 magenta, red or blue. (**A**-**C**) GFP and Vglut3 are present in largely separate populations,
1306 although some cells contain both proteins (one cell in this field, marked with an arrow).
1307 Two cells containing only GFP are indicated with arrowheads, and two cells containing
1308 only Vglut3 with double arrowheads. (**D**-**F**) There is a greater degree of overlap between
1309 GFP and Trpv1, and three double-labelled cells are shown with arrows. Some cells with
1310 only GFP or Trpv1 are indicated with single and double arrowheads, respectively. (**G**-**I**)
1311 GFP and somatostatin (Som) are found in separate populations, and some labelled cells
1312 are marked with single and double arrowheads, respectively. Note that somatostatin is
1313 seen as a partial ring around the nucleus in cells that express the peptide. (**J**-**M**) GFP cells
1314 often contain substance P (SP) but lack calcitonin gene-related peptide (CGRP), and 2 of
1315 these are marked with arrows. A single and double arrowhead mark cells with CGRP only
1316 and with both SP and CGRP, respectively. Scale bar: (**A**-**M**) = 100 μm.
1317

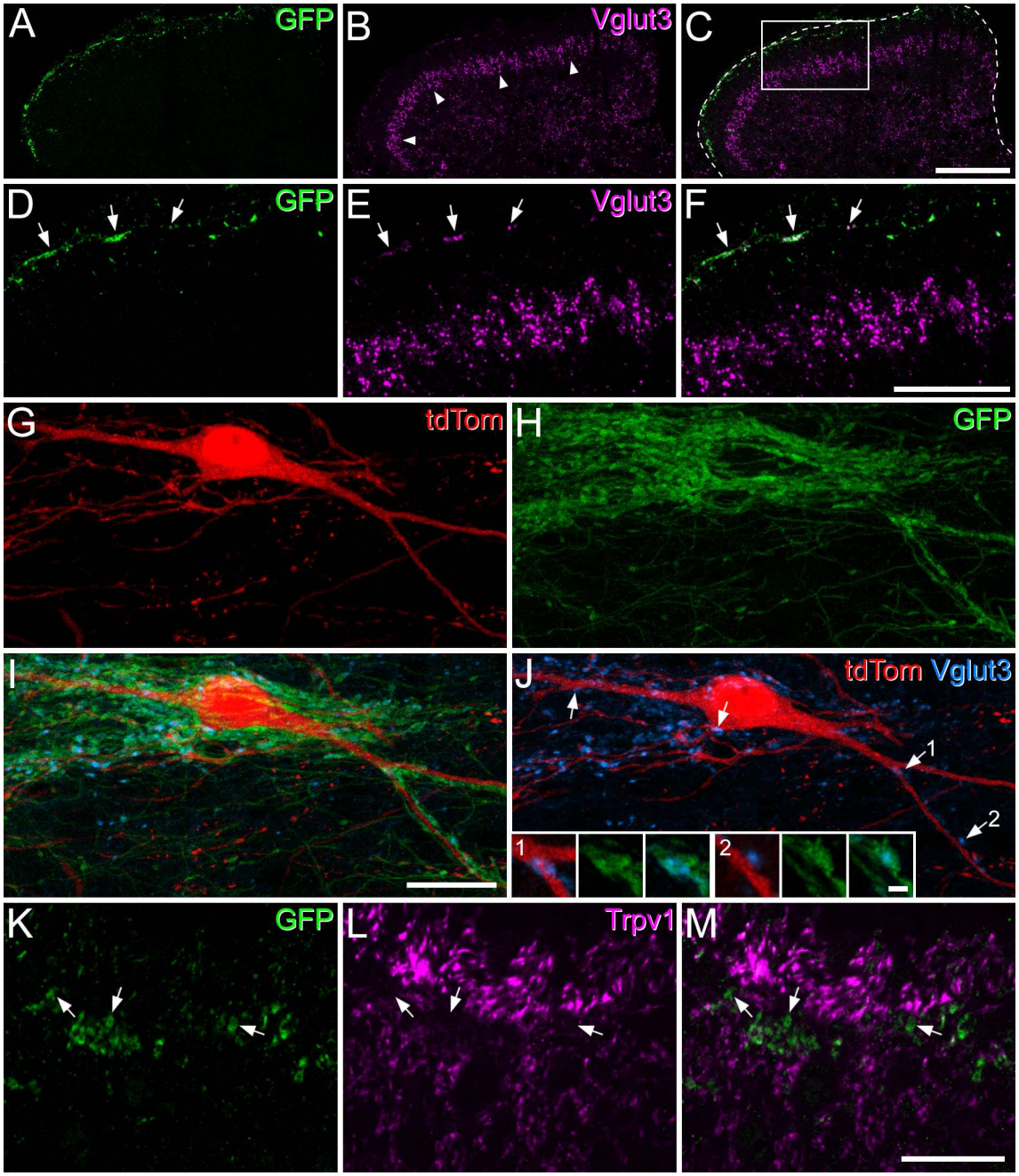

Figure 2–figure supplement 1. Expression of Vglut3 and lack of detectable Trpv1 in the central terminals of Trpm8 afferents. (**A**-**C**) A low magnification confocal image from a transverse section of the L2 segment in a Trpm8^{Flp};RCE:FRT mouse immunostained for GFP (green) and Vglut3 (magenta). GFP-labelled axons are restricted to lamina I, while a dense band of Vglut3-immunoreactive terminals in the inner part of lamina II (marked with arrowheads) corresponds to the central terminals of C low-threshold mechanoreceptors. The dashed line in C shows the outline of the dorsal horn and the box indicates the area shown in (**D**-**F**). (**D**-**F**) At higher magnification a few Vglut3 profiles are also seen in lamina

1327 I (arrows) and these co-express GFP. (**G**-**J**) A horizontal section through lamina I from a
1328 Phox2a::Cre;Ai9;Trpm8^{Flp};RCE:FRT mouse immunostained to reveal tdTomato (tdTom,
1329 red), GFP (green) and Vglut3 (blue). This field includes a tdTomato labelled projection
1330 neuron that receives numerous contacts from GFP-labelled axons. Some of these are also
1331 immunoreactive for Vglut3 and these are seen more clearly (some marked with arrows)
1332 when only tdTomato and Vglut3 are revealed (**J**). The insets in J show two of these Vglut3
1333 profiles (those marked with arrows numbered 1 and 2) contacting dendrites of the
1334 projection neuron in limited z-projections (2 optical sections at 0.5 µm z-spacing). In these
1335 images the coexpression of Vglut3 (blue) and GFP (green) is clearly visible. (**K**-**M**) A
1336 transverse section through lamina I from a Trpm8^{Flp};RCE:FRT mouse immunostained to
1337 reveal GFP (green) and Trpv1 (magenta). Although numerous Trpv1-immunoreactive
1338 profiles are visible, labelling for Trpv1 is generally not detected in the Trpm8 afferents,
1339 which express GFP. Scale bars: (**A**-**C**) = 100 µm, (**D**-**F**) = 50 µm, (**G**-**J**) = 50 µm, (**K**-**M**) =
1340 20 µm, (insets in **J**) = 2 µm.
1341
1342

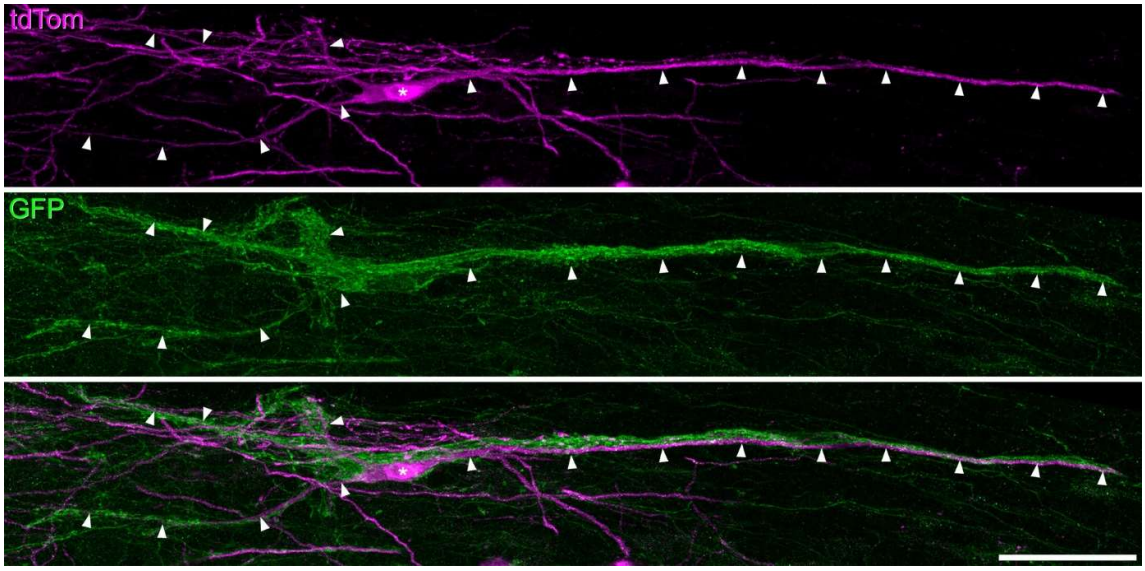

Figure 3–figure supplement 1. The relationship between tdTomato and GFP labelling for the cell illustrated in Figure 3. The top pane shows immunostaining for tdTomato (tdTom, magenta) in a horizontal section through lamina I from a Phox2a::Cre;Ai9;Trpm8^{Flp};RCE:FRT mouse. The tdTomato-labelled projection neuron illustrated in Figure 3 is visible. The soma is marked with an asterisk and parts of the dendritic tree with arrowheads. The cell body and dendrites are associated with dense bundles of GFP-labelled axons. Scale bar = 50 µm.

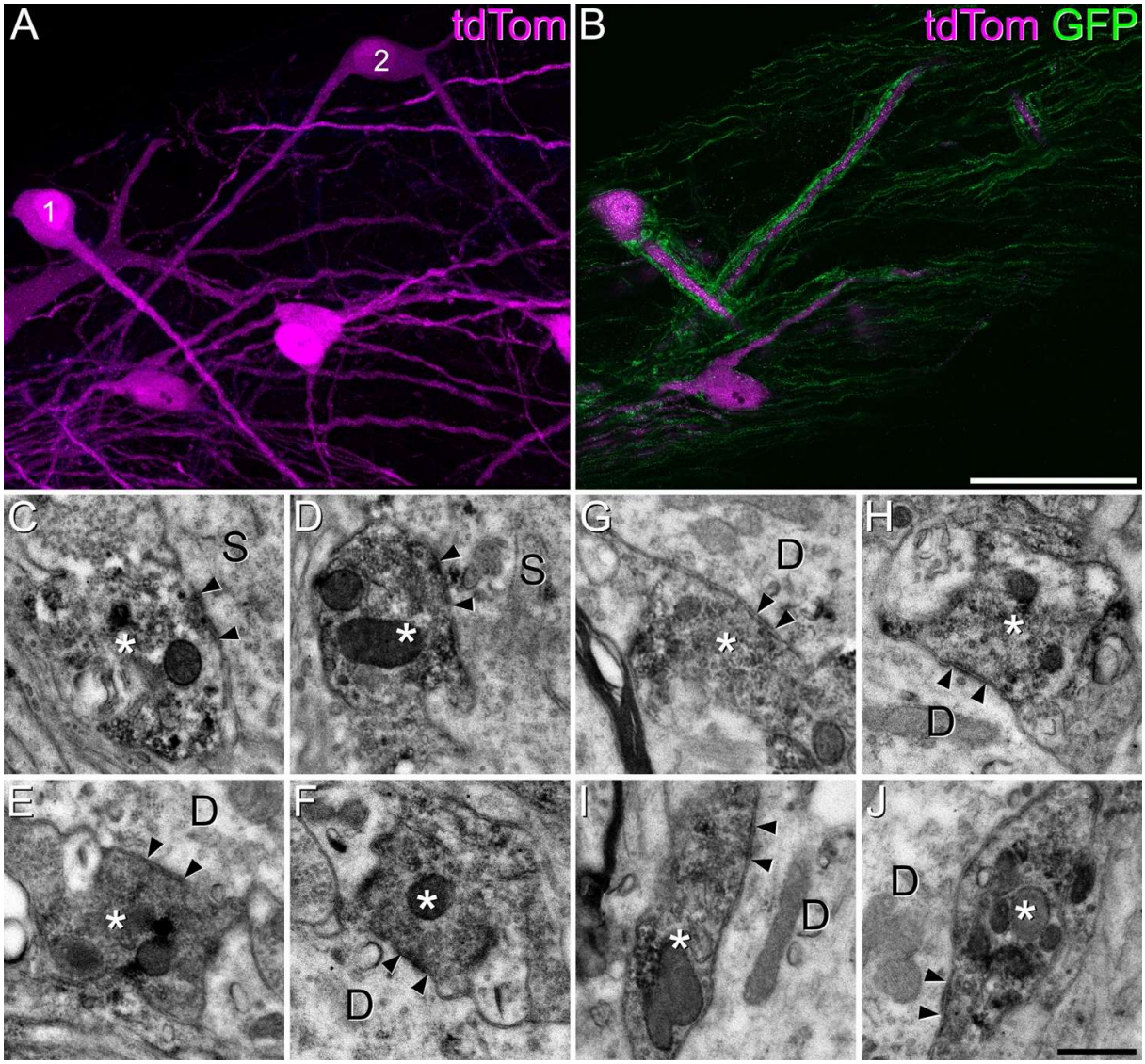

Figure 3–figure supplement 2. Confocal and electron microscope images of two Trpm8-innervated cells examined with the combined method in spinal cord sections from a Phox2a::Cre;Ai9;Trpm8^{Flp};RCE:FRT mouse. (**A**) Projected confocal z-stack showing parts of the two cells (numbered 1, 2) labelled with tdTomato (magenta) in a horizontal section. (**B**) a single optical section from the same confocal z-stack showing the association between axons labelled with GFP (green) and the cell body of cell 1 and dendrites of both cells. (**C-J**) Examples of synapses between the GFP-containing boutons, which are labelled with an immunoperoxidase method, and (unlabelled) dendrites (D) or soma (S) of the tdTomato-positive projection neurons. **C-F** show synapses on cell 1, and **G-J** those on cell 2. Presumed synaptic active zones (marked by arrowheads) can be recognised by the presence of vesicles on the presynaptic side and darkening of the

1367 membrane. However, these synapses do not show prominent postsynaptic densities.

1368 Scale bars: (**A**,**B**) = 50 μm, (**C**-**J**) = 500 nm.

1369

Click here to enter text.

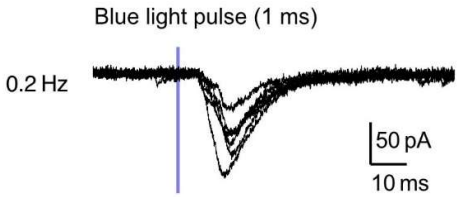

1370

1371 **Figure 3–figure supplement 3. Optogenetic evidence for possible polysynaptic input**
1372 **from Trpm8 afferents to a lamina I ALS cell with dense Trpm8 input** An example trace
1373 of an ALS cell with monosynaptic, and possibly also polysynaptic, inputs. Note that the
1374 delayed EPSCs exhibit latency jitter.

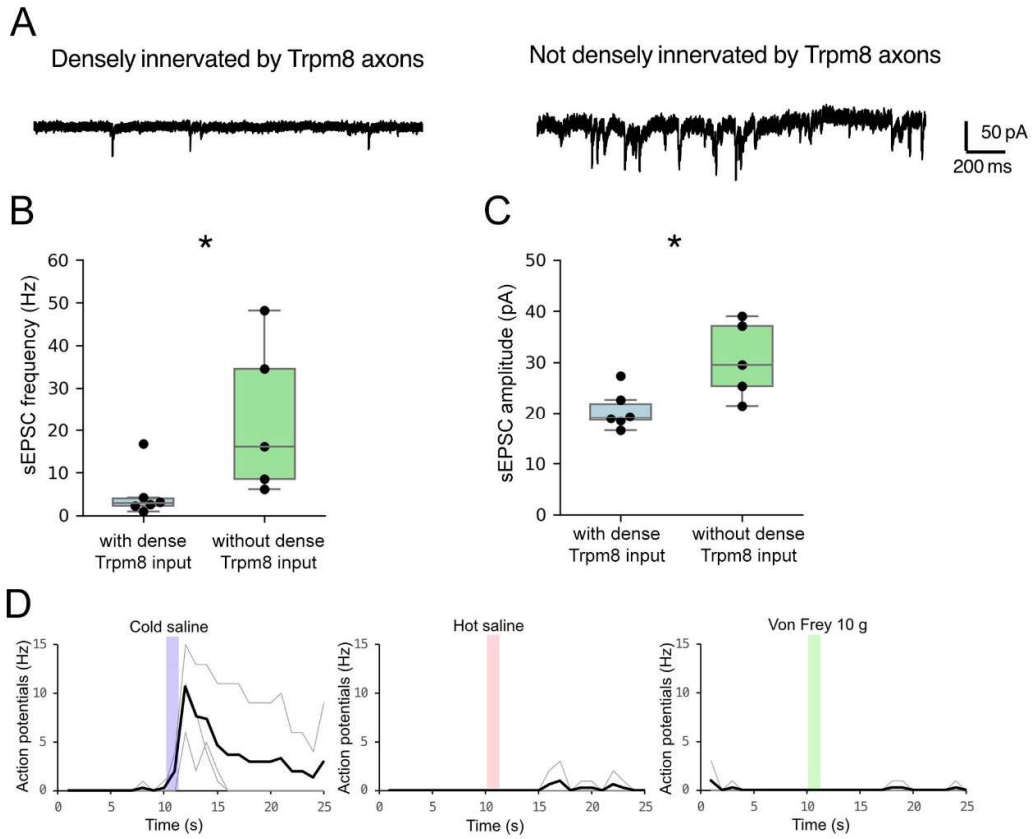

Figure 4–Figure supplement 1. Characteristics of spontaneous EPSCs in cold-selective and other lamina I ALS cells. (**A**) Representative traces from an ALS neuron with dense Trpm8 input (left) and an ALS neuron without dense Trpm8 input (right). (**B**,**C**) Quantification of sEPSC frequency (**B**) and amplitude (**C**) of ALS neurons. Box plots are median and interquartile range with symbols representing data points from individual ALS neurons (with dense Trpm8 input: n=6, without dense Trpm8 input: n=5; * indicates $p < 0.05$, Mann-Whitney U test). (**D**) Overlay of the firing time course of 3 cold-selective cells in response to cold, heat and mechanical stimulation. Note that action potentials frequency was determined from counts in 1 sec bins. Individual traces shown in grey and averages in black.

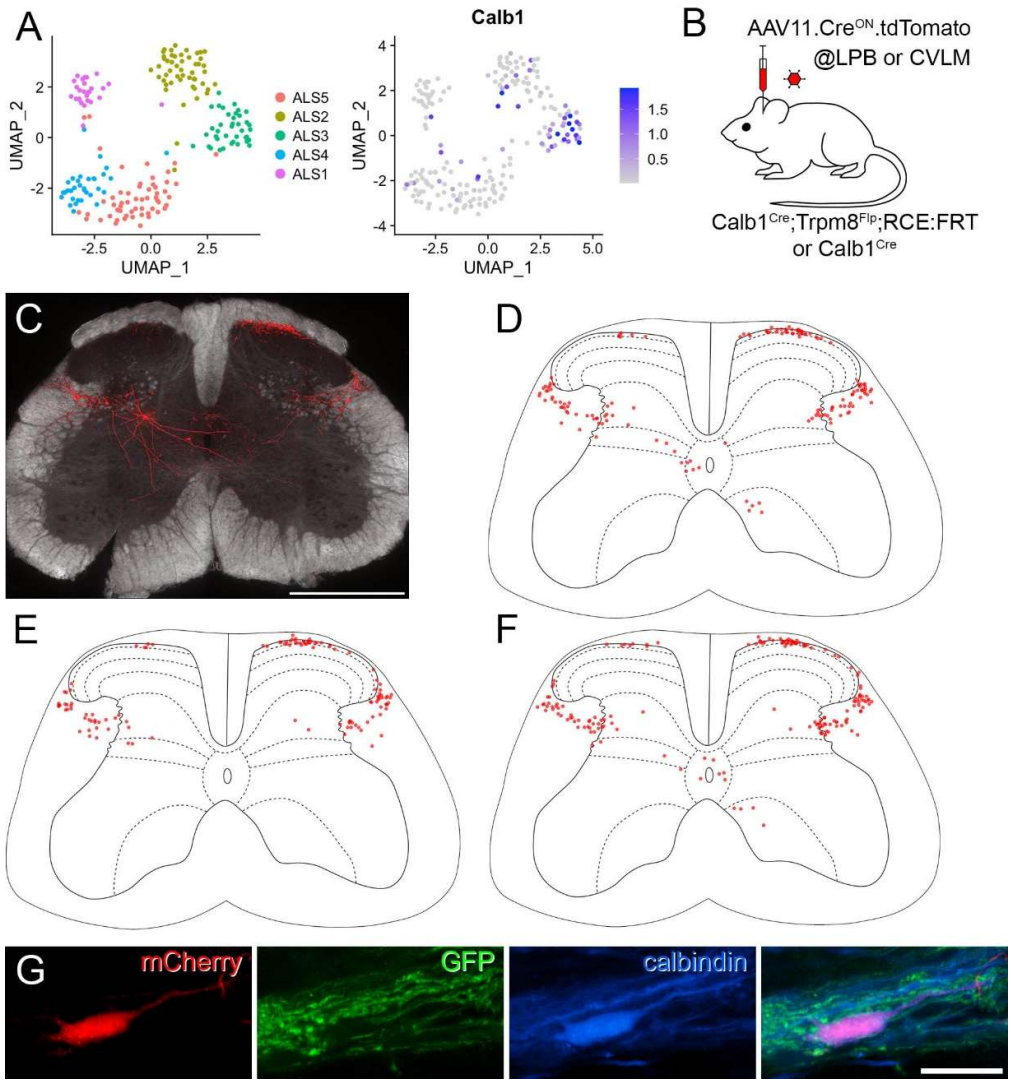

Figure 5–figure supplement 1. **Further characterisation of Calb1-expressing projection neurons.** (**A**) UMAP plot showing the distribution of cells in the ALS1-5 clusters, together with a plot for expression of Calb1. Note the presence of many Calb1-positive cells in the ALS3 cluster. (**B**) The experimental approach used to generate data presented in this figure and in Figure 5. (**C**) An example of a section through the L5 segment from a Calb1^{Cre} mouse injected with AAV11.Cre^{ON}.tdTomato in the LPB. Expression of tdTomato (red) is superimposed on a dark field image. (**D**-**F**) The distribution of retrogradely labelled cells in 9 (**D**,**F**) or 8 (**E**) transverse sections from the L5 segments of the remaining 3 Calb1^{Cre} mice injected with AAV11.Cre^{ON}.tdTomato in the LPB. The labelling for the other mouse is shown in Figure 5A. (**G**) Horizontal section through lamina I from the L4 segment of a Trpm8^{Flp};RCE:FRT mouse that had been injected with AAV9.mCherry into the LPB. The section has been immunoreacted to reveal mCherry

1400 (red), GFP (green) and calbindin (blue). A mCherry-positive lamina I neuron that is
1401 surrounded by GFP axons shows strong calbindin-immunoreactivity. Scale bar: (**C**) = 500
1402 μm, (**G**) = 20 μm.
1403

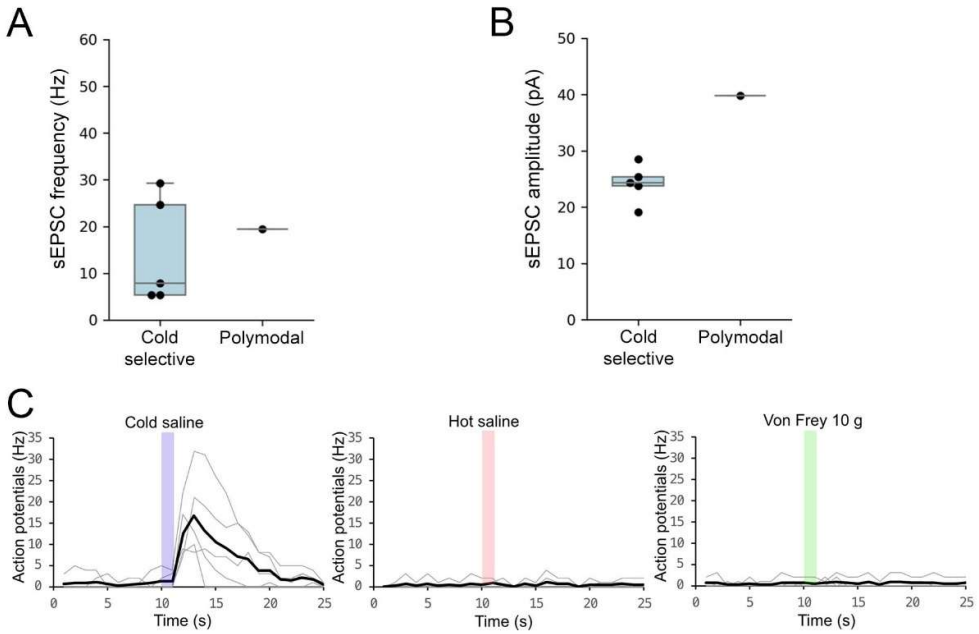

Figure 5–figure supplement 2. **Electrophysiological characterisation of Calb1-expressing projection neurons.** (**A, B**) sEPSC frequencies and amplitudes for the 5 cold-selective cells and the 1 polymodal cell recorded in Calb1^{Cre} mice injected with AAV11.Cre^{ON}.tdTomato in the CVLM. Note that although 2 of the cold-selective cells in this sample had relatively high sEPSC frequencies, when data from these cells were pooled with those reported for other sample of cold-selective cells (shown in Figure 4–Figure supplement 1) and compared with the polymodal cells shown in that Figure supplement, there was still a significant difference for both sEPSC frequency ($p = 0.037$) and amplitude ($p = 0.015$) (Mann-Whitney U test). (**C**) Overlay of the firing time course of 5 cold-selective cells in response to cold, heat and mechanical stimulation. Note that action potentials frequency was determined from counts in 1 sec bins. Individual traces shown in grey and averages in black.

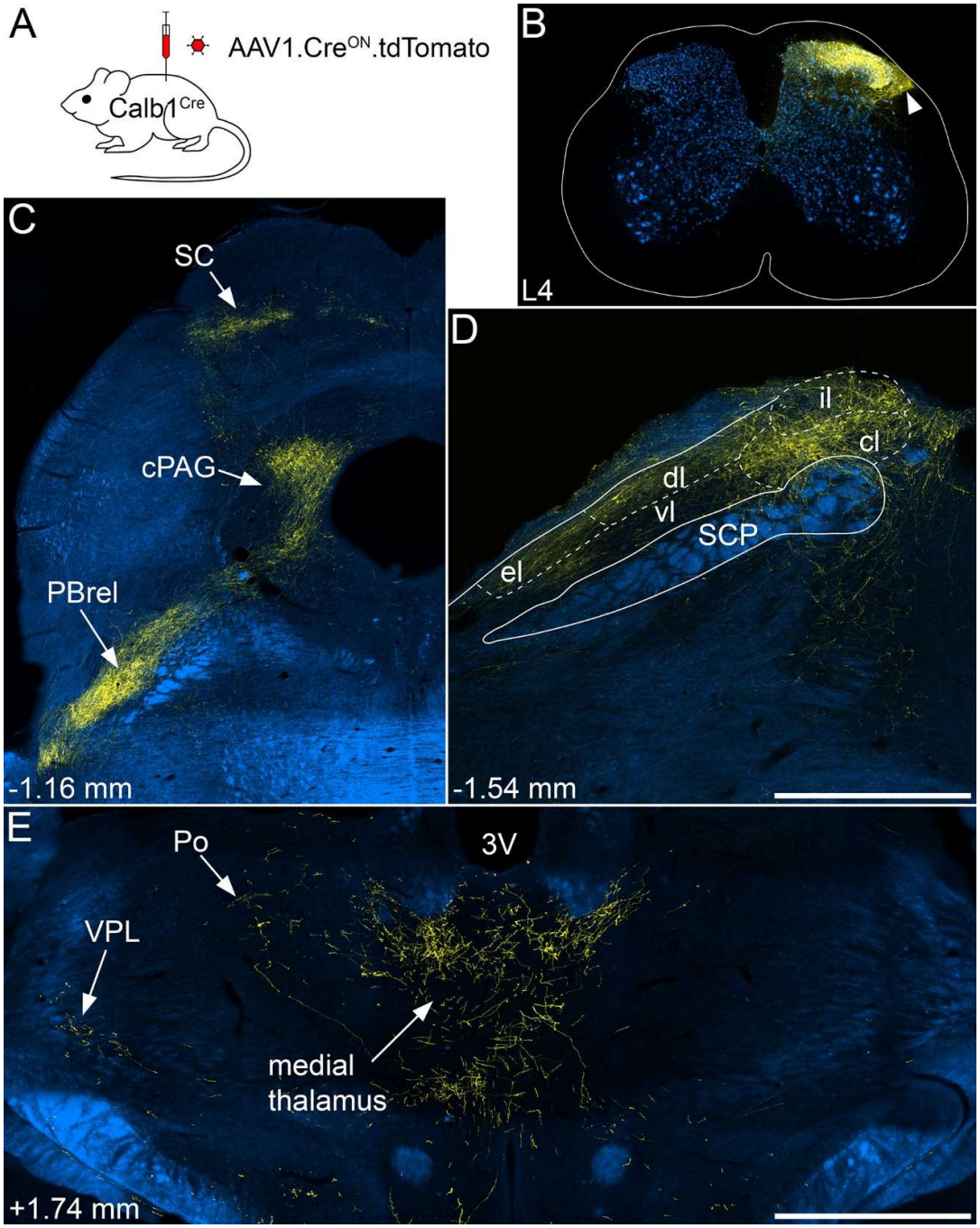

Figure 6–figure supplement 1. Anterograde labelling following injections of AAV1.Cre^{ON}.tdTomato into the central part of the spinal dorsal horn of Calb1^{Cre} mice. (**A**) The experimental approach used to generate data for Figure 6 and for Figure 6–figure supplements 1-3. Intraspinal injections were made into either the L3 or the L3, L4 and L5 segments, and were targeted on either the central or medial part of the dorsal horn. (**B**) Example of an injection into the central part of the L4 segment of a Calb1^{Cre} mouse. Immunostaining for tdTomato is shown in yellow and for NeuN in blue. There is extensive

1426 tdTomato labelling throughout most of the dorsal horn, and this extends into the lateral
1427 spinal nucleus (arrowhead), which contains tdTomato-labelled cell bodies. (**C**-**E**) Sections
1428 through selected regions of the brain have been immunostained to reveal tdTomato
1429 (yellow), and these are shown on corresponding dark-field images (blue). (**C**) There is
1430 strong labelling in the rostralmost part of the contralateral LPB, corresponding to the PBrel,
1431 as well as in the caudal PAG (cPAG). Unlike the pattern seen with injections restricted to
1432 the medial dorsal horn, there is also strong labelling in the contralateral superior colliculus
1433 (SC). (**D**) At a slightly more caudal level there is axonal labelling in several subnuclei of the
1434 contralateral LPB, including external lateral (el), dorsolateral (dl), central lateral (cl) and
1435 internal lateral (il), but not ventrolateral (vl). The location of the superior cerebellar
1436 peduncle (SCP) is indicated. (**E**) Within the diencephalon there is sparse axonal labelling
1437 in contralateral VPL and posterior (Po) thalamic nuclei, as seen following medial injections.
1438 However, there is also dense labelling in the medial thalamus, which was not seen with
1439 medial injections. Numbers in **C**-**E** show approximate rostrocaudal locations in relation to
1440 the interaural line. All images are from animal #2 in Table 1. Scale bars: (**B**,**C**,**E**) = 1 mm,
1441 (**D**) = 500 μm.
1442

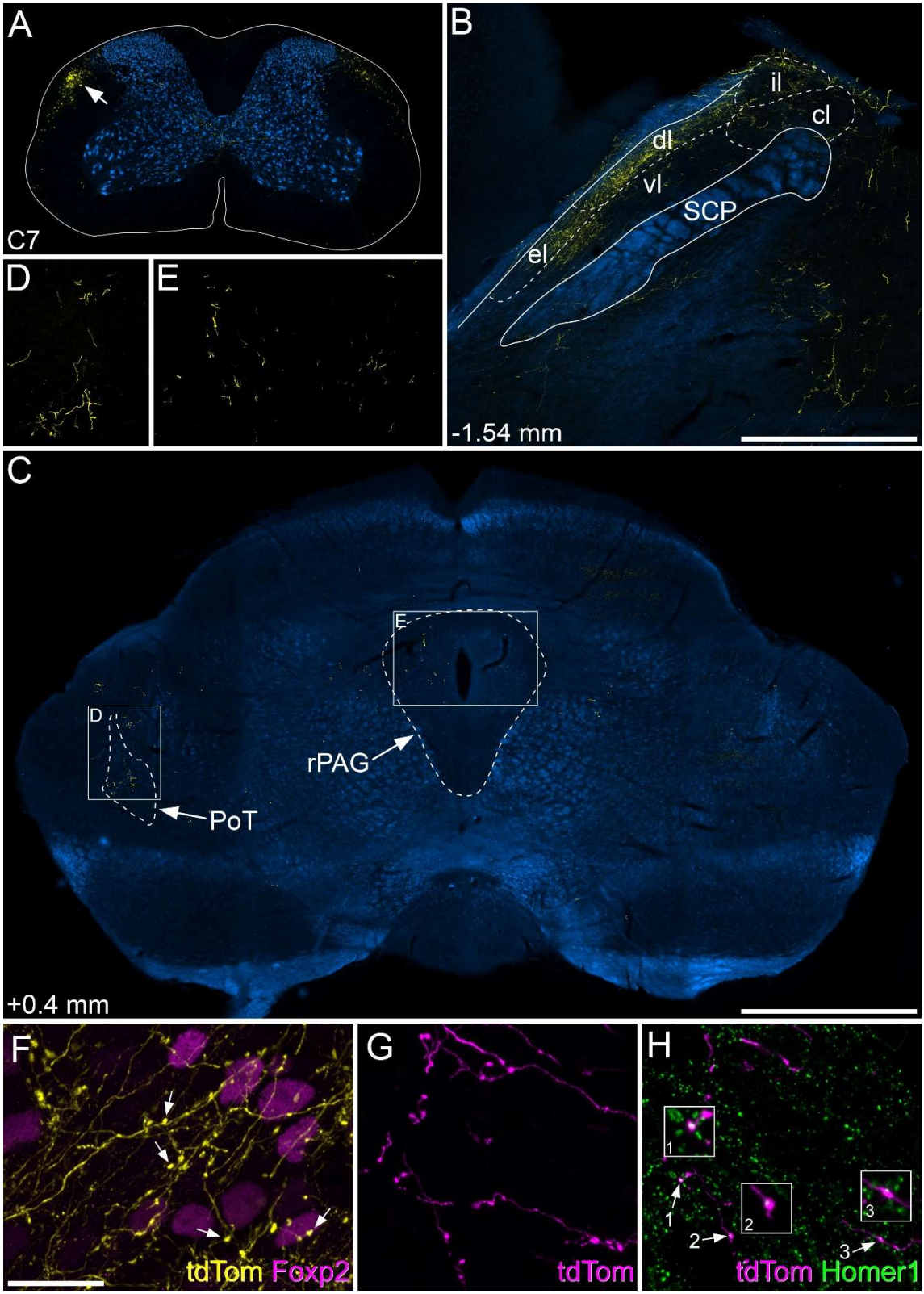

Figure 6–figure supplement 2. Anterograde labelling following injections of AAV.Cre^{ON}.tdTomato into the medial dorsal horn of Calb1^{Cre} mice. (**A**) A section through the C7 segment of a mouse that received injections into L3, L4 and L5 segments.

Click here to enter text.

1447 Immunostaining for tdTomato is shown in yellow and for NeuN in blue. There is a bundle of
1448 axons (arrow) in the contralateral dorsolateral white matter, with a much more weakly
1449 stained bundle in the same location on the opposite side. A few collateral branches are
1450 present in the deep dorsal horn and the area around the central canal. (**B**,**C**) Sections
1451 through selected regions of the brain have been immunostained to reveal tdTomato
1452 (yellow), and this is shown on corresponding dark-field images (blue). (**B**) At this level of
1453 the contralateral LPB, there is axonal labelling in the external lateral (el) and dorsolateral
1454 (dl) subnuclei, with very little labelling in ventrolateral (vl), central lateral (cl) or internal
1455 lateral (il). The location of the superior cerebellar peduncle (SCP) is indicated. (**C**) At a
1456 level corresponding to ~ 0.4 mm rostral to the interaural line there is very sparse axonal
1457 labelling in the posterior triangular nucleus of the thalamus (PoT) and in the rostral PAG
1458 (rPAG) on the side contralateral to the spinal injection. This is shown at higher
1459 magnification in (**D**) and (**E**), which correspond to the boxes in (**C**). (**F**) shows a maximum
1460 intensity projection of a z-series of 39 optical sections (0.5 µm z-separation) corresponding
1461 to part of the image shown in Figure 6G. Several varicosities, which probably correspond
1462 to synaptic boutons, are visible, and some are indicated with arrows. (**G**, **H**) High
1463 magnification views of anterogradely labelled axon terminals in the PBrel of a mouse that
1464 received injections into the L3, L4 and L5 segments. Immunostaining for tdTomato is
1465 shown in magenta and for Homer1 in green. The image in (**G**) is a maximum intensity
1466 projection from 23 optical sections at 0.5 µm z-separation, showing labelled axons with
1467 varicosities. (H) shows a projection of 3 optical sections (0.5 µm z-separation). Three of
1468 the varicosities in this field (arrows) are associated with Homer1 puncta and these are
1469 shown at higher magnification in insets. Note that the colour used to represent tdTomato
1470 has been altered to display the relation of Homer1 puncta to tdTomato varicosities.
1471 Numbers in **B** and **C** show approximate rostrocaudal locations in relation to the interaural
1472 line. Images in **A** and **C**-**E** are from animal #7, those in **B** and **F** are from animal # 8, and
1473 those in **G** and **H** are from animal #10 in Table 1. Scale bars: (**A**,**C**) = 1 mm, (**B**,**D**,**E**) = 500
1474 µm, (**F**-**H**) = 20 µm.
1475
1476

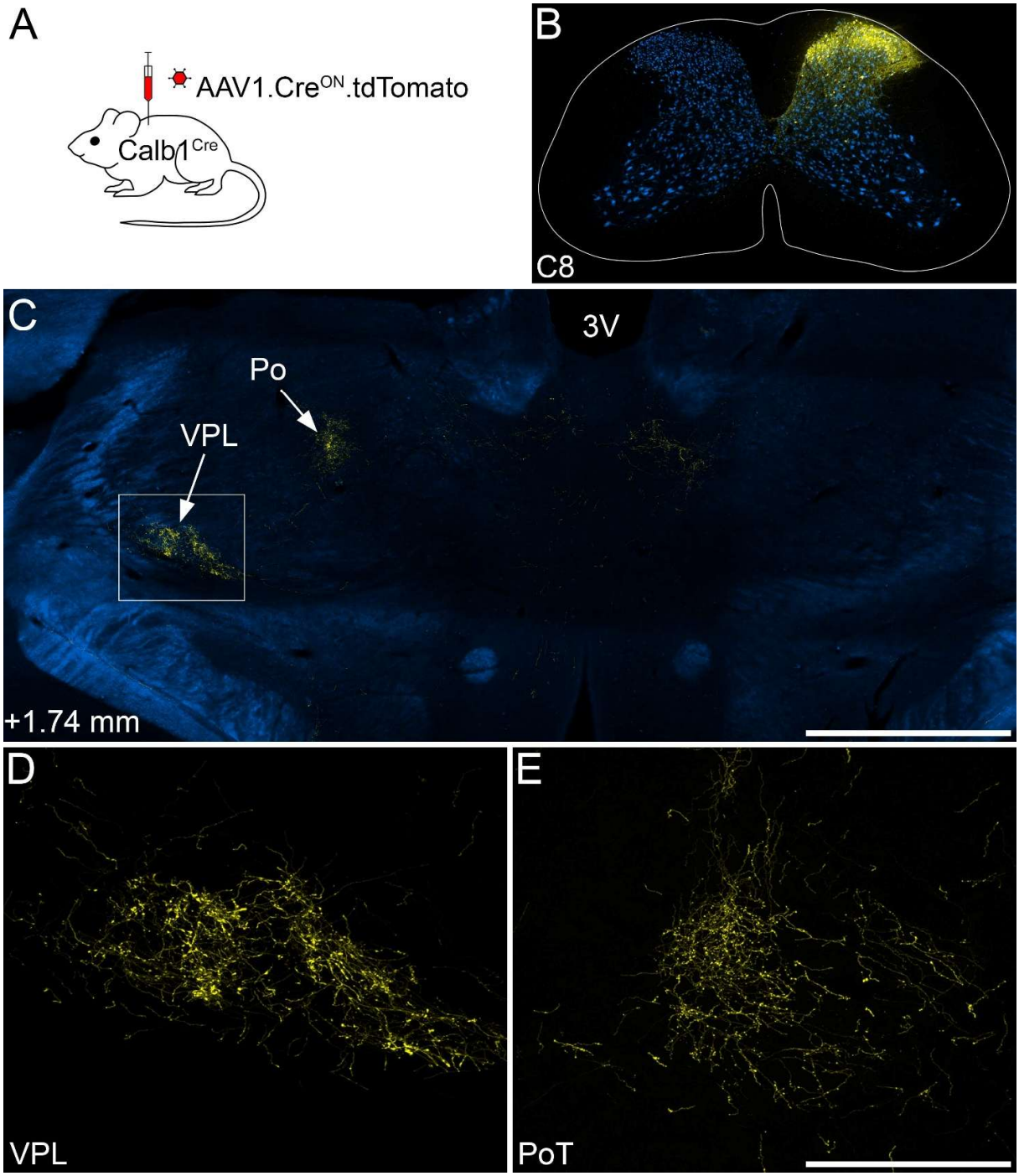

1477

1478 **Figure 6–figure supplement 3. Anterograde labelling following injections of**
1479 **AAV.Cre^{ON}.tdTomato into the cervical dorsal horn of Calb1^{Cre} mice** (**A**) The
1480 experimental approach used to generate data for this figure. Injections were made into the
1481 cervical enlargement. (**B**) Injection site in the C8 segment. Immunostaining for tdTomato is
1482 shown in yellow and for NeuN in blue. (**C**) A section through the diencephalon scanned to
1483 reveal tdTomato (yellow) and dark-field illumination (blue) shows dense tdTomato labelling

in the VPL and Po thalamic nuclei. The region in the box is shown at higher magnification in **D**. (**D**) Dense tdTomato labelling can be seen in the VPL. (**E**) At a more caudal level, there is also dense tdTomato labelling in the PoT nucleus of thalamus. The number in C shows the approximate location in relation to the interaural line. All images are from animal #14 in Table 1. Scale bars: (**B**,**C**) = 1 mm, (**D**,**E**) = 250 µm.

Click here to enter text.

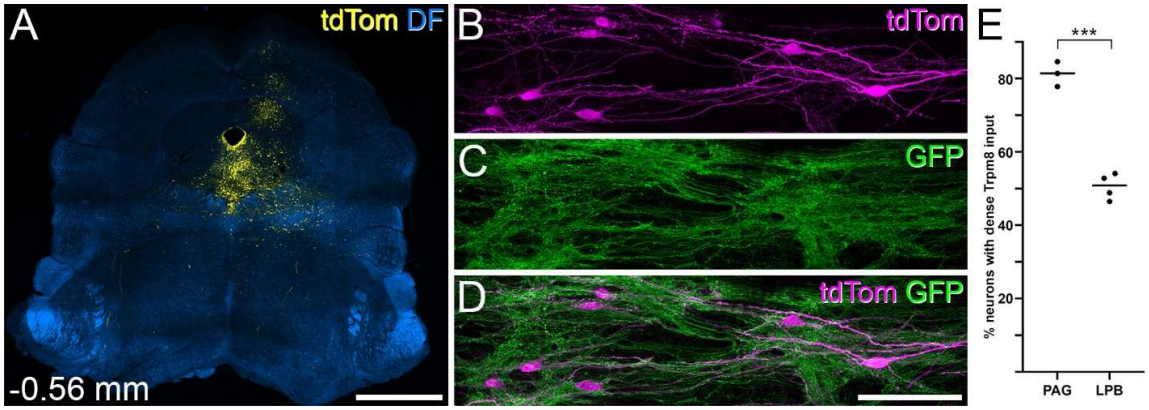

Figure 6–figure supplement 4. Retrograde labelling of Calb1-expressing ALS neurons from PAG. (**A**) TdTomato labelling at the site of injection of AAV11.Cre^{ON}.tdTomato in one of the 3 Calb1^{Cre};Trpm8^{Flp};RCE:FRT mice used in this part of the study. Note that this will not reveal the precise location of the injection, because only nearby Calb1-expressing cells will be labelled. (**B**-**D**) Labelling for tdTomato (tdTom) and GFP in a horizontal section through lamina I from the case illustrated in (**A**). Several tdTom-positive neurons are visible in this field, and all of them are densely coated with GFP-labelled (Trpm8-positive) axons. (**E**) Histogram showing the percentages of retrogradely labelled neurons in the L2-L4 segments that were densely coated with Trpm8-positive axons in this set of experiments (PAG), compared with the corresponding values from the 4 cases in which AAV11.Cre^{ON}.tdTomato was injected into the LPB. There was a highly significant difference between the percentages between the two injection sites ($p < 0.0001$, unpaired t-test with Welch's correction). Scale bars: (**A**) = 1 mm, (**B**-**D**) = 100 µm.

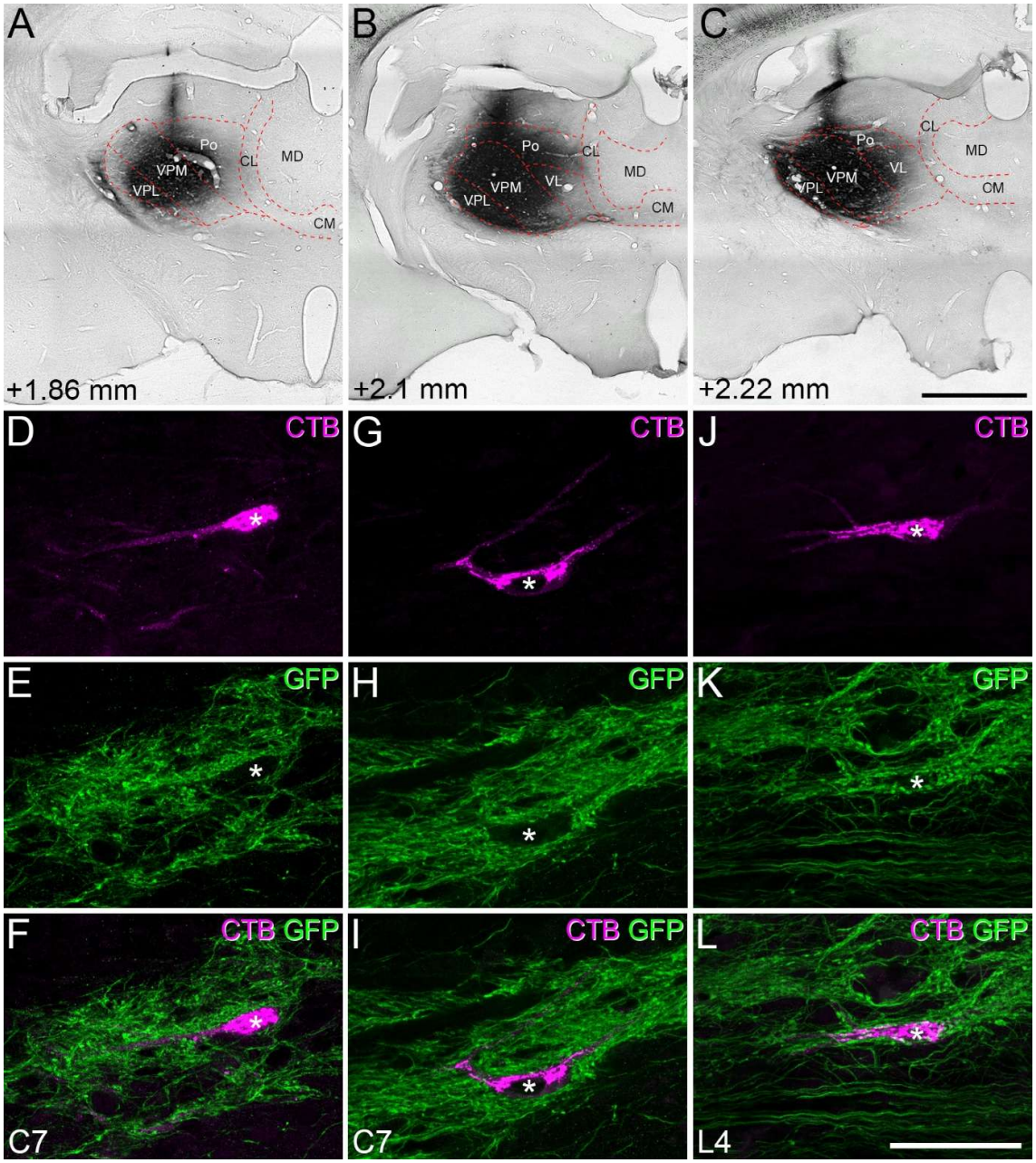

Figure 6–figure supplement 5. Identification of spinothalamic lamina I neurons with dense Trpm8 input. (**A-C**) CTB injection sites in the 3 experiments. In each case there is dense labelling in the ventral posterolateral (VPL) and ventral posteromedial (VPM) nuclei, together with some labelling in the posterior (Po) nucleus, and in two cases also in the ventrolateral (VL) nucleus. Note the lack of labelling in medial thalamic nuclei (centrolateral, CL; centromedial, CM; mediodorsal, MD). Numbers show approximate rostrocaudal locations in relation to the interaural line. (**D-I**) Examples of retrogradely labelled (CTB-positive) lamina I neurons (marked with asterisks) that are associated with numerous GFP-labelled (Trpm8-expressing) axons in horizontal sections through the C7

segments in the experiments illustrated in **A** and **B**. (**J**-**L**) In the experiment illustrated in **C**, we also identified 5 CTB-labelled cells in the L4 segment, and one of these, which is associated with numerous GFP-labelled boutons, is shown here (asterisk). Note that we also found CTB-labelled cells associated with numerous GFP-positive boutons in the C7 segment in this experiment. In each case, the images are shown below the injection site from the corresponding experiment. Scale bars: (**A**-**C**) = 1 mm, (**D**-**L**) = 50 μm.

Click here to enter text.

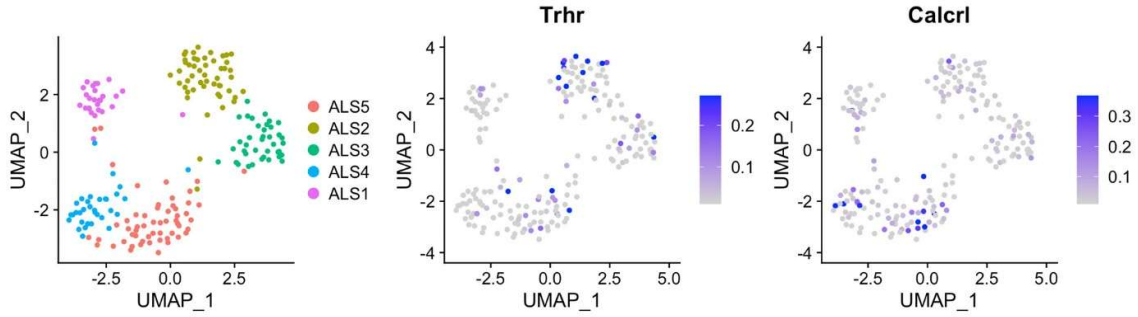

Figure 7–Figure supplement 1 UMAP plot showing the distribution of cells in the ALS1-5 clusters, together with plots for expression of Trhr and Calcrl. Note the presence of both Trhr and Calcrl in several of the ALS clusters, including ALS3.

1526 Table 1 Experimental details for Calb1^{Cre} mice used in anterograde tracing experiments.

1527

Animal	Sex	Injected segments	Injection location	Injection volume (nl)	Viral load (GC)	Survival (days)
1	M	L3, L4, L5	central	300	9.48×10^7	26
2	M	L3, L4, L5	central	300	9.48×10^7	55
3	F	L3, L4, L5	central	300	9.48×10^7	57
4	M	L3	central	300	9.48×10^7	42
5	F	L3	central	300	9.48×10^7	40
6	F	L3	central	300	9.48×10^7	40
7	M	L3, L4, L5	medial	150	4.74×10^7	55
8	M	L3, L4, L5	medial	150	4.74×10^7	54
9	F	L3, L4, L5	medial	150	4.74×10^7	41
10	F	L3, L4, L5	medial	150	4.74×10^7	55
11	F	L3	medial	150	4.74×10^7	41
12	F	L3	medial	150	4.74×10^7	41
13	F	L3	medial	150	4.74×10^7	53
14	M	C8	central	500	1.58×10^7	35
15	M	C8	central	500	1.58×10^7	44
16	M	C8	central	500	1.58×10^7	43

1528

1529 Mice received injections of AAV1.Cre^{ON}.tdTomato into the L3 segment only, the L3, L4 and
1530 L5 segments, or the C8 segments on the right side. Injections in lumbar cord were either
1531 targeted centrally (400 µm lateral to the midline) or medially (250 µm lateral to the midline)
1532 within the dorsal horn. Those in cervical cord were located centrally (430-450 µm lateral to

1533 the midline). All injections were made at 300 μm below the surface of the spinal cord.

1534 Injection volume and viral load refer to each injection in animals 1-3 and 7-9.